

**Methods for optimising immunohistochemistry for the serotonergic system in human
brainstem**

Steve Edwin
Integrated Program in Neuroscience
McGill University, Montreal
December 2021

A thesis submitted to McGill University in partial fulfillment of the requirements of the
degree of Master of Neuroscience

Table of Contents

Author's Contributions	04
Acknowledgements	05
Abstract	06
Résumé	07
Abbreviations	08
Chapter 1: Background Literature Review	09
1.1 Serotonin System in Primates	10
1.2 Antigen Retrieval Technique	16
Chapter 2: Rationale and Statement of Significance	19
2.1 Hypothesis	21
2.2 Objective	21
2.3 Specific Aim	22
Chapter 3: Research Methods	23
3.1 Sample acquisition and preservation	24
3.2 Ex-Vivo structural MRI scan	24
3.3 Tissue Sectioning and Preservation	25
3.4 Experimental Design – Heating water bath setup	27
3.5 Immunohistochemistry	28
3.6 Digitisation histological sections	32
Chapter 4: Results	33
4.1 Efficacy of HIER on tissue blocks and free-floating sections on IHC	37
4.2 Effect of high-pH and low-pH antigen retrieval buffers on the IHC	47
4.3 Optimise protocols to visualise the human 5-HT system using IHC	63
Chapter 5: Discussion and Conclusion	72
5.1 Discussion	73
5.2 Limitations	78
5.3 Conclusion	78
5.4 Perspective - Serotonin, Atlases and Parkinson's Disease	79
References	85

This work is dedicated to my family, my pillar of support, in helping me navigate a very challenging time of my life.

AUTHOR'S CONTRIBUTION

The experimental design, planning and execution of the experiments for the master's thesis project were completed by myself under the supervision of Dr. Sadikot. Conceptualisation of the project was done with the guidance of my supervisor, Dr. Sadikot. Experimental work consisting of tissue processing, antigen retrieval processing, immunohistochemistry and image acquisition were performed by myself, under Dr. Sadikot's supervision. The preliminary stage of tissue block generation was performed with the help of two colleagues, Dr. Prajakta Ghate and Jemal Yesuf, working at the Cone lab. The relevant background literature review, the methodological approach, presentation of the results with concluding remarks, relevant discussion and the possible implications of the study, were compiled and written by myself and reviewed by Dr. Sadikot as part of the master's thesis document.

ACKNOWLEDGEMENTS

This work is the outcome of a very challenging three years of my life. Amid a pandemic with a unique situation in my scientific career, with the grace of God and the help of my loved ones, I am grateful to be able to successfully present this work.

I would first like to thank my mom, dad and sister for their constant, untiring support during this exceptionally challenging time. From being there, patiently listening to all my troubles, to wisely helping me navigate them, I am eternally grateful to them for always being there and giving me the strength to take the tough decisions.

I would also like to thank my friends Zahraa and Prajakta for being there when I needed them the most. I would also like to express my gratitude to my committee members – Dr. Christine Tardif, Dr. Jean-Francois Cloutier and my mentor, Dr. Edith Hamel for guiding me in completing my thesis with their patience and understanding. I owe a special thanks to the IPN team - Dr. Edward Ruthazer, Ms. Viviane Omune and Mirko Sablich who all greatly helped me in navigating my final year at McGill within their respective capacities.

And lastly, I would like to thank my supervisor, Dr. Abbas Sadikot for his supervision and in providing me with the opportunity for a learning experience that has certainly transformed me. I would also like to thank Dr. Vladimir Rymar and my lab mates in helping to maintain a cheerful work environment.

ABSTRACT

Understanding the anatomical organisation of a neuronal system provides critical insight into its possible functions [Frazer A. et al., 1999]. The serotonergic system is involved in the modulation of a diverse spectra of behaviours; from cardiovascular and respiratory functions to stress responses, appetite, sleep, locomotion, learning, memory, aggression, and reproductive functions [Azmitia E. C., 1999; Soiza-Reilly M. & Gaspar P., 2020]. Identification of the various subsets of the serotonin raphe nuclei using specific morphological, chemical, and molecular markers will provide insight into the role of these subsets in diverse physiological functions such as stress, memory, locomotion, and sleep cycles.

The current subdivisions of the serotonergic neurons for primates rely on correlating its cellular localisation with that of the subdivisions of the raphe nuclei, identified in the rodent brainstem (B1-B9 nomenclature; Dahlström A. & Fuxe K., 1964) based on Nissl staining. This proves to be a significant challenge for studies looking at structure-function relationships in the serotonergic system, as the raphe nuclei of the brainstem are composed of ill-defined aggregates of neurons which flank the midline and contain most of the serotonergic neurons [Bach H & Arango V et al., 2012].

Although immunohistochemistry is currently the best available technique to visualise and determine the ground truth of a neurotransmitter system using post-mortem tissue, it requires significant tissue and cellular marker specific standardisation. With the following study, I aim to lay the groundwork for overcoming these discrepancies with regards to serotonergic cell counts, their projection patterns, and classification in human tissue by developing an optimal visualisation methodology for the human serotonergic system using immunohistochemistry. To that end, with this systematic study, I have examined various methods and developed the most optimal immunohistochemical protocol for the visualisation of the serotonergic system in post-mortem human brain and identified the possible pitfalls, with a focus on antigen retrieval techniques.

Keywords : Serotonin, Antigen retrieval, Primates, Immunohistochemistry, Tryptophan hydroxalase-2, Serotonin transporter (SERT), Atlases, Chemical Anatomy

RÉSUMÉ

Comprendre l'organisation anatomique d'un système neuronal fournit un aperçu critique de ses fonctions possibles [Frazer A. et al., 1999]. Le système sérotoninergique est impliqué dans la modulation d'un spectre diversifié de comportements ; les fonctions cardiovasculaires et respiratoires, les réponses au stress, l'appétit, le sommeil, la locomotion, l'apprentissage, la mémoire, l'agressivité et les fonctions de reproduction [Azmitia E. C., 1999; Soiza-Reilly M. & Gaspar P., 2020]. L'identification des différents sous-ensembles des noyaux de sérotonine du raphé, à l'aide de marqueurs morphologiques, chimiques et moléculaires spécifiques, fournirait un aperçu du rôle de ces sous-ensembles dans diverses fonctions physiologiques telles que le stress, la mémoire, la locomotion et les cycles du sommeil.

Les subdivisions actuelles des neurones sérotoninergiques des primates reposent sur la corrélation de sa localisation cellulaire avec celle des subdivisions des noyaux du raphé identifiés dans le tronc cérébral des rongeurs (nomenclature B1-B9; Dahlström A. & Fuxe K., 1964), basée sur la coloration de Nissl. Cela s'avère être un défi important pour les études portant sur les relations structure-fonction dans le système sérotoninergique, car les noyaux du raphé du tronc cérébral sont composés d'agrégats de neurones mal définis qui flanquent la ligne médiane et contiennent la plupart des neurones sérotoninergiques [Bach H & Arango V et al., 2012].

Bien que l'immunohistochimie soit actuellement la meilleure technique disponible pour visualiser et déterminer le fonctionnement fondamental d'un système de neurotransmetteurs à l'aide de tissus post-mortem, elle nécessite une standardisation importante des tissus et des marqueurs cellulaires. Dans l'étude suivante, je vise à surmonter ce conflit, spécifiquement concernant le nombre de cellules sérotoninergiques, leurs modèles de projection et leur classification dans les tissus humains, en développant une méthodologie de visualisation optimale pour le système sérotoninergique humain avec l'immunohistochimie. À cette fin, avec une étude systématique, j'ai examiné diverses méthodes et développé le protocole immunohistochimique le plus optimal pour la visualisation du système sérotoninergique dans le cerveau humain post-mortem, et identifié les limites possibles, en mettant l'accent sur les techniques de récupération d'antigènes.

Mots clés : Sérotonine, Recherche d'antigène, Primates, Immunohistochimie, Tryptophane hydroxalase-2, Transporteur de sérotonine (SERT), Atlas, Anatomie chimique

ABBREVIATIONS

CL _i	Caudal linear nucleus
DRN	Dorsal raphe nucleus
MRN	Medial raphe nucleus
PH8	Anti-phenylalanine hydroxylase antibody
PH8-ir	PH8-immunoreactive
PFA	Paraformaldehyde
DA	Dopamine
NA	Noradrenaline
5-HT	Serotonin
GFP	Green-fluorescent protein
SLC6A4	Solute carrier family-6 member-4 gene
HIER	Heat-induced epitope retrieval
TPH	Tryptophan hydroxylase
TPH1	Tryptophan hydroxylase – 1
TPH2	Tryptophan hydroxylase – 2
PBS	Phosphate buffered saline
PETS	Paraffin embedded tissue slices
IHC	Immunohistochemistry
BSA	Bovine serum albumin
HRP	Horseradish peroxidase
ABC	Avidin-biotin complex
DAB	3,3'-diaminobenzidine
SERT or 5-HTT	Sodium dependent serotonin transporter
PMR	Paramedian raphe nucleus
NRTP	Nucleus reticularis tegmenti pontis
NRPO	Nucleus reticularis pontis oralis
PT	Pyramidal tract
RM _g	Nucleus raphe magnus
Gi	Gigantocellular nucleus
V _L	Ventral laminae of the principal olive
STN	Subthalamic nucleus

CHAPTER 1: BACKGROUND LITERATURE REVIEW

1.1 Serotonin System in Primates

The central serotonergic system in vertebrates is involved in the modulation of a diverse spectra of behaviours; from cardiovascular and respiratory functions to stress responses, appetite, sleep, locomotion, learning, memory, aggression, and reproductive functions [Azmitia E. C., 1999; Soiza-Reilly M. & Gaspar P., 2020]. These widespread and diverse effects of serotonin are attributed to its diffuse anatomical organisation with highly collateralised axons [Berger M., Gray J. A., & Roth B. L., 2009; Azmitia E. C., 1999]. Even though serotonin fibers innervate almost every region of the central nervous system, their cell bodies are few and are arranged as discrete cell clusters located along the brainstem midline [Frazer A. et al., 1999; Charnay Y., & Léger L., 2010] with a very restricted organisation in the hindbrain, the raphe nuclei [Azmitia E. C., 1999]. For the last six decades, various techniques have been used to characterise the serotonin neuronal circuitry [Charnay Y., & Léger L., 2010]. The advent of immunohistochemical techniques in combination with anterograde and retrograde tracing studies [Muzerelle A., et al., 2016; Halberstadt A. L., & Balaban C. D., 2007], have allowed for a better approximate characterisation of the cell bodies and afferents of the serotonin system in the CNS when compared to the initial underestimation using histochemical/fluorescence stains [Frazer A. et al., 1999] which suffered from limited sensitivity.

Historically, the subdivision of the serotonergic neurons relied on correlating topographic localisation with that of the subdivisions of the raphe nuclei, identified in the rodent brainstem (B1-B9 nomenclature; Dahlström A. & Fuxe K., 1964). But as this classification relied on earlier descriptions of the raphe nuclei based on Nissl staining, identification of the serotonergic system remained incomplete with possibly many false positives and negatives affecting the downstream classification schemes. This is especially challenging as the raphe nuclei of the brainstem are composed of ill-defined aggregates of neurons which flank the midline and contain most of the serotonergic neurons [Bach H & Arango V et al., 2012]. The raphe, divided into rostral and caudal projection groups, [Törk I. & Hornung J P., 1990; Hornung J P., 2003] consists of the caudal linear nucleus (CL_i), dorsal raphe nucleus (DRN) and medial raphe nucleus (MRN) in the rostral group and raphe magnus nucleus, raphe obscurus, raphe pallidus nucleus comprising the caudal group. But many neuronal cell bodies are found outside of the raphe nuclei and include the presence of many non-serotonergic cells within them [Frazer A. et al., 1999; Halliday G. M. & Törk I., 1986; Sladek J. R. Jr et al., 1982; Poitras D., & Parent A., 1978]. For example, the CL_i group that is present in the ventral

mesencephalic tegmentum contains Substance P (SP) and pigmented dopaminergic neurons interspersed with the serotonergic neurons [Halliday G. M. & Törk I., 1986]. Most of the neurons present in the raphe nuclei are non-serotonergic in nature, with serotonin cells only comprising between 40-50% of the total cell bodies within the DRN, the largest serotonin containing raphe nuclei [Frazer A. et al., 1999].

The B1-B9 nomenclature of the serotonin neurons, which refers to the topography along the hindbrain anteroposterior axis of the rodent brainstem, only partially coincides with the modern classifications based on single cell analysis [Soiza-Reilly M. & Gaspar P., 2020; Okaty B. W. et al., 2015]. Even though these subdivisions are used across mammalian and rodent species alike, they show significant variations with respect to size and the relative extent of the lateralisation of the subgroups [Muzerelle A. et al., 2016; Shimogori T. et al., 2018; Parent M. et al., 2011; Wallman M. J. et al., 2011].

Serotonin-containing cell body groups	Anatomical structure
B₁	Raphe pallidus nucleus, caudal ventrolateral medulla
B₂	Raphe obscurus nucleus
B₃	Raphe magnus nucleus, rostral ventrolateral medulla, lateral paragigantocellular reticular nucleus
B₄	Raphe obscurus nucleus, dorsolateral part
B₅	Median raphe nucleus, caudal part
B₆	Dorsal raphe nucleus, caudal part
B₇	Dorsal raphe nucleus principal, rostral part

B₈	Median raphe nucleus, rostral main part; caudal linear nucleus; nucleus pontis oralis
B₉	Nucleus pontis oralis, supralemniscal region

Table 1: Serotonergic cell body group classification based on Dahlström A. & Fuxe K. (1964) and their respective anatomical regions delineated in rodent systems [Frazer A. et al., 1999].

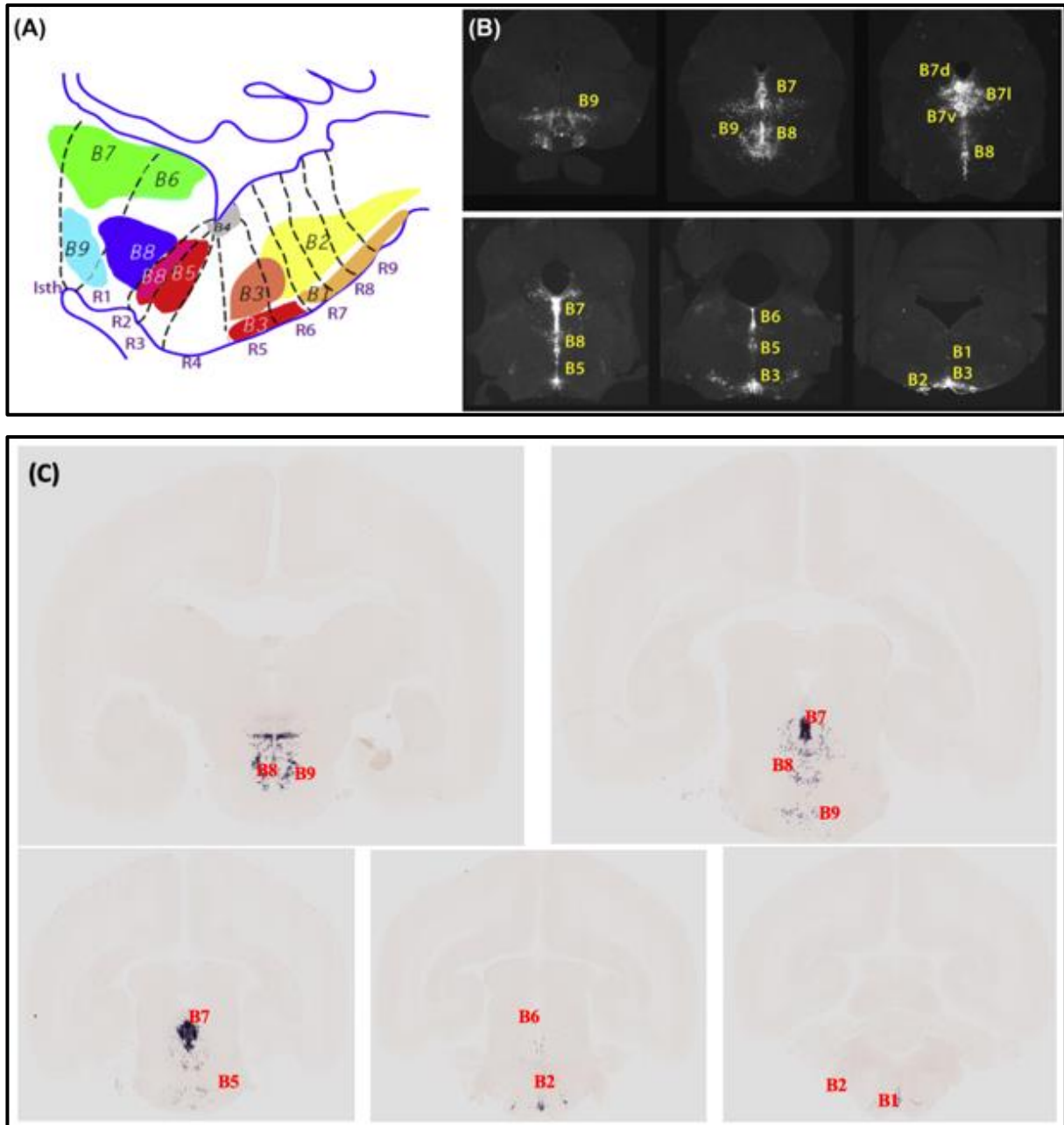
The rostral serotonergic system, comprising the DRN, MRN and the B₉ cell groups, form the ascending projection system. This ascending system emerges in two distinct fashions – along the dorsal periventricular path and via the ventral tegmental radiations [Frazer A. et al., 1999]. These two pathways converge at the level of the hypothalamus, merging with the medial forebrain bundle, coursing anteriorly alongside the dopaminergic and noradrenergic fibers [Frazer A. et al., 1999]. From the limited studies, the topographical organisation of the ascending projections has been documented [Parent M. et al., 2011; Wallman M. J. et al., 2011]. The striatum & the hippocampus receive extensive projections from the DRN while the MRN projects to the septum & hypothalamus [Frazer A. et al., 1999]. The DRN and MRN cell groups organised in unique zones project distinctively to specific brain regions [Frazer A. et al., 1999]. Brain regions that are related in function receive axon collaterals from the raphe neurons, such as the amygdala & hippocampus and the substantia nigra & the caudate putamen [Frazer A. et al., 1999]. Along with the subthalamic nucleus (STN), thalamus, globus pallidus, striatum, and the cortex they form the core structures of the cortico-basal ganglia-thalamocortical loop, disruption of which are involved in the pathophysiology of neurodegenerative disorders such as PD [Huot P. et al., 2011]. Instead of a global non-specific “neuromodulator” role presumed to be played by serotonin, these highly specific and organised innervation patterns indicate towards independent functions by the different sets of serotonin neurons. Topography, cellular properties, origin, and terminal projections of serotonergic neurons seem to significantly affect their role in the manifestation of affective disorders [Okaty B. W. et al., 2015].

At present, it is not possible by tract-tracing methods to verify the cortical targets of the various DRN & MRN nuclear subdivisions in humans [Bach H. & Arango V. et al., 2012], even though it has been known for decades that there are massive projections arising from the raphe to the telencephalon [Taber E., Brodal A., & Walberg F. 1960]. The dual ascending serotonergic projection systems were hence only systematically described in rats [Mamounas L. A. et al., 1991] and non-human primates [Wilson M. A., & Molliver M. E., 1991(a), (b)]. The fibers found to originate from the DRN, named D-type fibers illustrate a fine, varicose axonal system that branches profusely in the target area [Bach H. & Arango V. et al., 2012]. The M-type fibers on the other hand, found to selectively originate from the MRN, have large round varicosities and a more divergent innervation. It has also been observed that these two fiber-types project and distribute variably in the rat cortex [Kosofsky B. E. & Molliver M. E., 1987]. Also intriguingly, it has been noted that the fine D-type fibers are significantly more susceptible to amphetamine derivatives, while the M-type fibers seem to be spared [Wilson, M. A. et al., 1989].

Using early anatomical descriptions in rodents and non-human primates, the evidence that had accumulated for the need to differentiate serotonin neurons based on function and regulation has now recently been reinforced and validated using molecular, physiological, and multidimensional single-cell analyses [Okaty B. W. et al., 2015]. Developmental trajectories, molecular identities, physiological properties, and connectivity patterns are some recent additions to the subclass identification criteria. But currently, this subclass identity is based on cytoarchitectonic & topographic features alone [Baker K. G., 1990]. Interestingly, on subsequent validation of the cytoarchitectonic and topographic classification of the serotonergic neurons using a chemical marker, anti-phenylalanine hydroxylase (PH8) sera [Törk I. & Hornung J. P., 1990; Hornung J. P., 2003; Bach H. & Arango V. et al., 2012], previously unrecognised additional serotonin cell groups were discovered, for example the *ventral subnucleus*. This nucleus which was found to have the highest density of PH8-ir neurons [Olszewski J. & Baxter D. et al., 1954] was not accounted for when using Nissl based cytoarchitectonic methods, as that is a crude approximate method for quantifying the neurons of a neurotransmitter system.

Now, PH8 in itself is not an ideal immunohistochemical marker to visualise the serotonergic neurons as it is a marker against phenyl-alanine hydroxylase, tyrosine hydroxylase and tryptophan hydroxylase, secondary enzyme structures present in all monoaminergic systems

[Sigma-Aldrich, Product-MAB5278, Clone PH8, Chemicon®, Mouse]. The challenge with using non-specific antibodies to label serotonin cell bodies which has been the norm (i.e., PH8), is that it also identifies the DA and NA cell types. This antibody relies on significant PFA penetration and the generation of cross-links to mask the detection of DA and NA by the PH8 antibody. This method of localising serotonin cell types, based on the epitope masking ability of PFA, is not accurate as the masking capabilities of PFA cannot be quantified.



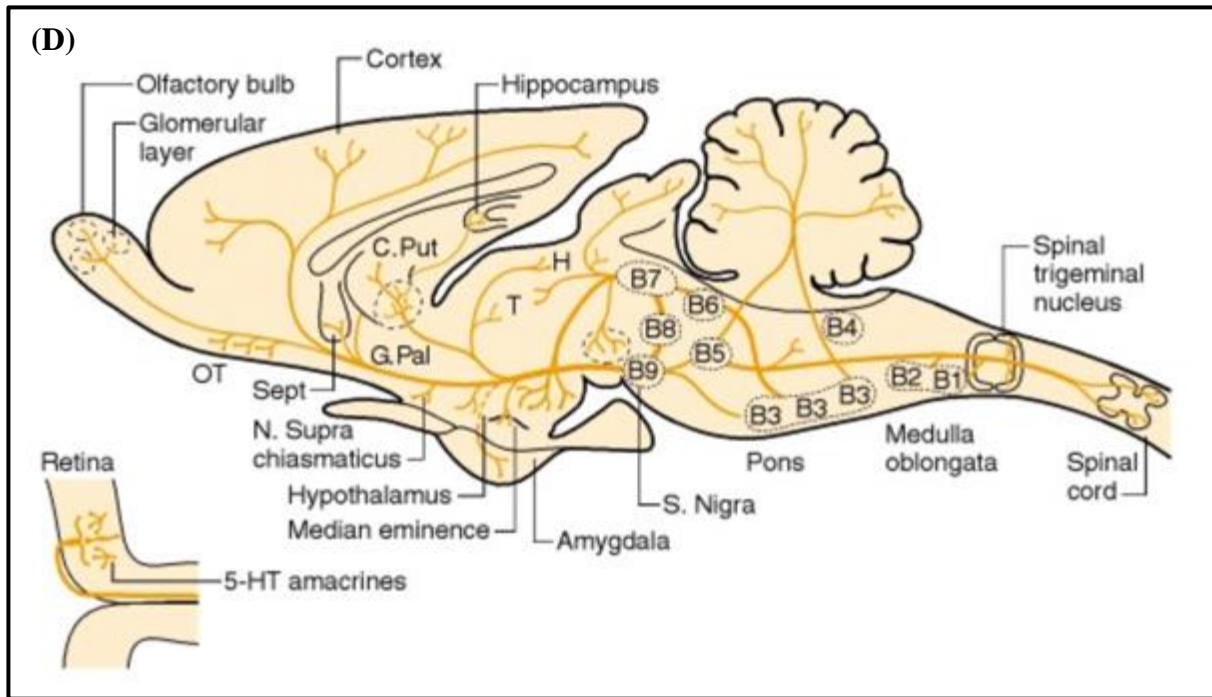


Figure 1: (A & D) A schematic view of the distribution of the B1-B9 serotonergic cell group topography in the rodent system. (B) Serial coronal sections of a P7 mouse brain in which 5-HT raphe neurons were genetically labeled with GFP (Pet1-Cre mice were crossed to a conditional GFP reporter line). (C) SERT expression in the primate brain (SLC6A4 gene expression pattern). Coronal sections of a P0 marmoset brain labeled for SERT by in situ hybridization. (B) Adapted from: Muzerelle, A., Scotto-Lomassese, S., Bernard, J. F., Soiza-Reilly, M., & Gaspar, P. (2016). Conditional anterograde tracing reveals distinct targeting of individual serotonin cell groups (B5-B9) to the forebrain and brainstem. (C) Data obtained from: (<https://gene-atlas.brainminds.riken.jp>) Shimogori, T., Abe, A., Go, Y., Hashikawa, T., Kishi, N., Kikuchi, S.S., et al. (2018). Digital gene atlas of neonate common marmoset brain. *Neuroscience Research*, 128, 1-13. (D) Adapted and modified from Consolazione, A., and Cuello, A. C. CNS serotonin pathways. In *The Biology of Serotonergic Transmission*. New York: John Wiley & Sons, Ltd., 1982, pp. 29–61.

Understanding the neuroanatomical organisation of a neuronal system provides critical insight into its possible functions [Amunts K., Mohlberg H. et al., 2020; Frazer A. et al., 1999]. Identification of the various subsets of the serotonin raphe nuclei using specific anatomical, chemical, and molecular markers will provide insight into the role of these subsets in diverse physiological functions such as stress, memory, locomotion, and sleep cycles. Supporting this, recent electrophysiological studies of the serotonin neurons of rodent system found further

evidence for functional diversity in the regulation of behaviours, including regional specificity within the DRN itself [Crawford, L. K. et al., 2010].

These discrepancies with regards to serotonergic cell counts, their projection patterns, and classification in human tissue, hindered by the lack of an optimal visualisation methodology using post-mortem tissue must be addressed. Immunohistochemistry is currently the best available technique for post-mortem tissue in visualising and determining the ground truth with regards to the organisation of the serotonergic system. A systematic study for the development of an optimal immunohistochemical protocol for its visualisation is therefore required. Here, based on initial suboptimal results, I propose to examine different methods for optimising the immunohistochemical protocol in post-mortem human brain with a focus on antigen retrieval techniques.

1.2 Antigen Retrieval Technique

Over the last four decades, visualisation of antigens using immunohistochemical methods in human brain tissue have been significantly limited by the masking effects of fixatives such as formaldehyde [Alelú-Paz R. et al., 2008]. Fixation is the process of preserving a biological molecule by changing its shape, introducing cross-links, preventing its degradation via endogenous peroxidases or microbial enzymes while enabling the molecule to withstand the rigors of tissue processing by locking in the secondary structure [Alelú-Paz R. et al., 2008] and retaining excellent tissue morphology.

Standardisation and quality control of immunohistochemical techniques critically depend on antigen-retrieval techniques and their method of application [Shi S. R., Shi Y., & Taylor C. R., 2011; Tacha D. & Teixeira M. 2013]. The lack of standardisation of this critical technique across antibodies makes it imperative for the end-user to develop and optimise the protocols for immunohistochemistry specifically for the target epitopes. Antigen-retrieval is a preprocessing measure used to prepare the sample tissue for downstream immunohistochemical processing [Shi S. R., Cote R. J., & Taylor C. R., 1997; Shi S. R., Shi Y., & Taylor C. R., 2011]. This is a vital step in producing uniform staining across the entire tissue by limiting regional variability, increasing the efficiency of the antibodies used, reducing the revealing time for the target regions and in significantly reducing non-specific background noise. Most tissues in a histopathology laboratory are fixed in formalin or 4%

paraformaldehyde which introduces cross-links between epitopes or within them and may inadvertently mask these epitopes, preventing antibody access [Karlsson C., & Karlsson M. G., 2011; Tacha D. & Teixeira M. 2013]. But such cross-links can be reversed with the application of heat and buffered solutions. To that end, a wide range of buffered solutions at various pH (low and high) applied at different temperatures have been developed over the years. But these buffered solutions, pH, temperature, and duration of the retrieval buffer application is extremely antibody specific and not standardised [D'Amico, F., Skarmoutsou, E., & Stivala, F., 2009]. Further validating the critical nature of this pre-IHC step are studies that have compared archival studies performed on paraffin embedded blocks before the onset of antigen retrieval methods to the results obtained with antigen retrieval on similar blocks. These studies confirmed the role of the appropriate antigen retrieval method in eliminating false negatives and improving the immunostaining quality. Such studies also showed that extremely sensitive antibodies that had only previously worked with frozen tissues also performed equally well with formalin-fixed tissues after antigen retrieval [Cuevas E. C. et al., 1994].

Sharma *et al.* (1990) showed the earliest use of heat-induced antigen retrieval (HIER) technique, improving immunoperoxidase staining with 23 different antibodies, using a microwave oven setup. This was followed by Shin *et al.* (1991) and Shi *et al.* (1991), where they used an autoclave with distilled water as the immersion liquid and lead thiocyanate in a microwave setup respectively to improve the immunoreactivity of formalin-fixed, paraffin embedded tissues [Tacha D. & Teixeira M. 2013]. Over the years, safer buffers that produced consistent results which are not as harsh on the tissue specimen were developed by various groups – 0.01M citrate buffer (pH 6.0) [Cattoretti G. et al., 1993], EDTA [Morgan J. M. et al., 1994]. The sensitivity of antibodies differed across the various buffers, with each antibody having a unique preference.

This resulted in the lack of a universal retrieval buffer that is optimally applicable to all tissue epitopes. The unique chemical nature of each buffer utilises their characteristic properties for the optimal unmasking of the target epitopes [Krenacs L. et al., 2010; Ramos-Vara J. A., 2017]. Properties of temperature, pH, buffer, molarity, and other additional components significantly affect the same [Magaki S. et al., 2019]. Of the routinely used retrieval buffers in histopathology laboratories, low-and high-pH buffers, EDTA-and Tris-based buffers are the most frequently used [Krenacs L. et al., 2010; Ramos-Vara J. A., 2017]. Citrate based buffers

are the most common of them all, due to its gentle treatment of the tissues because it works well for most common epitopes. But it does not unmask antigens that have extensive cross-links and does not provide optimal staining for them. For low tissue expression antigens or over-fixed tissues, harsher retrieval buffers of higher pH, temperature and stronger buffers must be used [Stumptner C. et al., 2019].

Raising tissue temperature is another important factor in the unmasking of the epitopes. Standard range of temperatures used range between 60°C - 100°C for tissue blocks or slices [D'Amico, F., Skarmoutsou, E., & Stivala, F., 2009]. The challenge with using tissue slices at higher temperatures includes the possibility of tissue shrinkage, distortion, an increase in the brittleness of the tissue and an inclusion of folds or wrinkles in the tissue slice. But this disadvantage is offset by quality uniform unmasking across the entire tissue slice, enabling the downstream immunohistochemistry to represent the ground truth results contained in the target region. Using a tissue block reverses the dynamic and presents the possibility of having non-uniform unmasking of the epitopes leading to differential staining in the tissue which would misrepresent the regional variability inherent in the target regions. But this significant disadvantage comes at the benefit of the preservation tissue morphology and structural integrity of the native tissue block, enabling precise reconstructions of the tissue blocks from its slices.

Staining intensity is directly proportional to the time and temperature the tissue is subjected to [Tacha D. & Teixeira M. 2013], with longer time and higher temperatures producing intense staining. Water bath, steamer, pressure cookers, microwaves and autoclaves are few of the instruments that have been tested to successfully subject the tissue pre-treatment [Tacha D. & Teixeira M. 2013]. Specific limitations associated with the various devices include those of time taken to achieve critical temperature, evaporation, heating artefacts due to overheating and tissue damage [Tacha D. & Teixeira M. 2013]. Systematic optimisation and standardisation of the antigen retrieval methods pertaining to specific serotonin antibodies must be performed to achieve consistent, uniform results in the quest to visualise the serotonergic system in human tissue effectively and accurately.

CHAPTER 2: RATIONALE AND STATEMENT OF SIGNIFICANCE

Histologically, the serotonergic system remains one of the most understudied monoaminergic systems due to the significant challenges associated with studying it in human brain specimens. Identifying the serotonergic cell groups based on its chemical profile has been a significant challenge in human brain tissue due to the rapid dissipation of serotonin (5-HT) from the neurons after death [Wallman M.J. et al., 2011; Parent M. et al., 2011]. Morphological studies of the serotonergic system must rely on different indirect markers - serotonin-associated proteins as such as the serotonin synthesising enzyme (tryptophan hydroxylase - TPH), serotonin transporter (SERT) or serotonin receptors. Studies have shown that the isoform tryptophan hydroxylase-2 (TPH2) is present in nervous tissue whereas TPH1 has a more peripheral distribution [Walther D. J. et al., 2003; Zhang X. et al., 2004]. However, the limited studies that have used TPH as a marker have only studied the presence of TPH1 in non-human primate brain specimens. This under-samples the neurons presenting the TPH profiles. Using the correct TPH isoform, i.e., TPH2, a more accurate representation of the serotonergic profile in human brainstem would be depicted. Although it provides excellent visualisation of the serotonergic cellular and proximal dendrite distribution patterns, it is significantly limited in terms of fiber staining. Serotonin transporter (SERT) provides an alternative avenue in trying to visualise the fiber projections [Nielsen K. et al., 2006; Vertes R. P. et al., 2010]. But due to the diffuse, varicose nature of the serotonergic projections, using SERT to visualise the fibers presents its own challenges [Raghanti M. A. et al., 2008].

To address these challenges, with this project, I propose to investigate, identify & resolve the pitfalls, compare various approaches & protocols, and develop the most optimal working protocol for the creation of a serial histological dataset of the serotonergic system with specific chemical markers in a human hemi-brain specimen using an immunohistochemical approach to be able to be used for quantitative stereological analysis.

Antigen retrieval is a standard procedure for enhancing immunohistochemical detection [Shi S. R., Shi Y., & Taylor C. R., 2011]. With the wide range of antigen retrieval techniques out there, it is crucial to identify and choose the method that works specifically for the antibody of interest. Serotonergic systems have been understudied, at times using antibodies for immunohistochemistry that may be inappropriate. This is so because of the intense background staining that is observed with serotonin, again due to the intense, global, and diverse innervation patterns of the serotonergic system. Using non-specific antibodies to label serotonergic cell bodies have been the norm. For example, (PH8), which labels serotonergic

cell bodies but also identifies DA and NA cell types [**Sigma-Aldrich, Product-MAB5278, Clone PH8, Chemicon®, Mouse**]. This antibody relies on significant PFA penetration and generation of cross-links to mask the detection of DA and NA cells by the PH8 antibody. This method of localising serotonin cell types is not accurate as the masking capabilities of PFA cannot be quantified and regional variabilities in PFA penetration would exist. Due to the challenges associated with visualising SERT in a specific region, its regional innervation pattern appears as patches of serotonin reactivity instead of very defined patterns of innervation in terms of fiber bundles or specific fiber systems.

In trying to address these issues, I aim to identify the optimal antigen retrieval protocols for the serotonergic system antibodies (TPH2 and SERT-IS). As part of the creation of a histological dataset, the comparative efficacy of antigen retrieval techniques when applied to tissue blocks and tissue slices will also be systematically studied.

2.1 HYPOTHESIS

With the application of optimal antigen retrieval techniques, a specific targeted reduction in background staining, increased fiber tract visibility, reduced non-specific targeting, reduced staining by endoperoxidases and increased antibody efficiency will be achieved.

2.2 OBJECTIVE

The overarching objective of this project is to standardise the various stages for the immunohistochemical acquisition of a high quality, low distortion histological dataset of the human serotonergic system at a laboratory scale. This standardised immunohistochemical protocol can then be applied to the creation of serotonergic volumetric datasets in healthy, ageing, and specific neurodegenerative systems such as PD to have a disease specific histological atlas and for performing quantitative stereological analysis. While many aspects are required for standardisation, in this thesis I will focus on examining optimal methods for antigen retrieval and in developing an optimal immunohistochemical protocol for the serotonergic system.

2.3 SPECIFIC AIM

AIM: Compare and optimise heat-induced antigen retrieval techniques & protocols on tissue blocks and free-floating sections prior to being subjected to standard immunohistochemical techniques.

- (A) Determination of the comparative efficacy of HIER protocol on tissue blocks and free-floating sections*
- (B) Determination of the effect of high-pH and low-pH antigen retrieval buffers on the IHC staining*
- (C) Standardise and develop an optimal protocol for the visualisation of serotonergic cell bodies and fiber tracts by modifying standard immunohistochemical protocol.*

CHAPTER 3: RESEARCH METHODS

3.1 Sample acquisition and preservation

Following autopsy, the brains were weighed and immediately transferred into the fixative solution of 4% paraformaldehyde in phosphate buffered saline (PBS, pH 7.4) for immersion fixation. With a mid-sagittal cut, the two hemispheres were separated, and the left hemisphere was collected for the analysis. This hemisphere was maintained at 4°C until further processing. Three fiducial markers were placed in the hemisphere before ex-vivo structural MRI scans were performed. These fiducial markers were determined using 3T T1 MRI scans of the brain. Marks along the anterior limb of the internal capsule, the external capsule and the posterior limb of the internal capsule were placed prior to the 7T MRI scans of the hemisphere. Following the 7T scan, blocks containing; a) the pons, medulla, cerebellum, and b) the basal ganglia, mesencephalon and diencephalon were generated.

The first block was trimmed off by removing the cerebellum in a coronal plane at the level of the posterior tip of the fastigium of the fourth ventricle. The regions of interest for the second block were selectively collected by cutting the block along the level of the anterior and posterior ends of the corpus callosum in a coronal fashion. The temporal and parietal lobes were removed from the block by making a sagittal cut at 4.5 cm lateral to the interhemispheric midline and by making a horizontal cut through the middle part of the trunk of the corpus callosum respectively.

Identifier	Sex	Age	4% PFA Fixation Duration	Cause of Death	Specimen Available
Brain 1	M	45	21 months	Cocaine induced cardiac myopathy	Left hemisphere, brainstem
Brain 2	M	72	14 months	Gastric Carcinoma	Left hemisphere

Table 1: Clinical data on the donor brains used for the study. The post-mortem brains were collected and preserved for the purpose of creating ultra-high-resolution atlases.

3.2 Ex-Vivo Structural MRI Scan

After removing the brains from the fixative overnight and placing the fiducial markers, the hemispheres were transferred into MRI compatible containers with fluorinert™ FC-40 (Sigma, CAS#51142-49-49-5). This MRI compatible fluid was used to reduce susceptibility artifacts that may present during MRI scans. The containers were tapped gently to remove any air bubbles. A high field 7T MRI scan of the hemisphere (Pharmascan) was performed followed by a small-bore 7T MRI scan of the blocks to acquire structural T1 and T2 weighted images. These images were scanned over approximately 16 hours for the hemisphere 7T and 18 and 21 hours approximately for the brainstem and basal ganglia 7T blocks respectively. After acquisition of the MRI scans, the brain blocks were immersed in a fresh fixative solution for 24 hours and then transferred to 30% sucrose solution.

3.3 Tissue Sectioning and Preservation

Using a manual precision sliding microtome (MICROM, USA) that was fitted with a custom specimen stage and cooling system, brain blocks were cut into 50µm thin sections. The stage temperature was held between -12°C and -15°C. Blocks were mounted on the stage that was covered with finely crushed dry ice to achieve a uniform freezing across the block. Agarose mounds were used to keep the block in place. Sections were cut in axial plane, parallel to the AC-PC line. Block face images were taken at every 6th section for both the blocks. Individual sections were collected separately in serially labelled six-well plates which was filled with PBS (pH 7.4) and was stored in a 4°C fridge immediately after cutting. For long term storage, the sections were transferred to an anti-freeze solution (30% ethylene glycol, 30% glycerol, 0.2M phosphate buffer pH 7.4), that was kept at 4°C overnight and then stored at -20°C until further use.

Subcortical block generation and histological section acquisition protocol from a human hemi-brain.

(A) Generation of the Basal Ganglia and Brainstem Block along the AC-PC line

Block-face images are collected after every 300 µm i.e., every 6th section. Block-faces images are a crucial intermediary, helping in the eventual development of co-registration methods for

the histological dataset to the MRI dataset. The photographs were taken at the beginning of the microtome sledge course, with the brain in the exact same position section after section [Dauguet J. et al., 2007]. On average, a series of 2000 images are obtained at an in-plane resolution of 0.08 mm x 0.08 mm. Photographs were taken with the following settings – Manual exposure (exposure bias = 0), exposure time = 1/3, flash off, focal length = 105, auto white balance, focus distance = 0.668, normal contrast, DPI = 300 x 300, Image dimensions = 6144 x 4912 and ISO = 63.

(B) Embedding protocol for 50 µm thick slice sectioning using a freezing microtome

Histological 3D reconstruction assumes that the sections generated by volume slicing are uniform and change smoothly across the sections which unfortunately is not true. Serial sections usually suffer from various artefacts which occur independently of each other and affect each slice differently. One of the most critical steps is the acquisition of thick tissue slices where the maximal number of irreversible artefacts are generated, affecting tissue quality greatly and in turn significantly impacting the subsequent steps. The two of the most common methods of generating thick tissue sections are – paraffin embedded sectioning and by using a frozen microtome. But both these techniques carry significant limitations.

To generate paraffin embedded tissue slices (PETS), the tissue block needs to be subjected to extensive pre-processing - dehydration, clearing and impregnation only following which the tissues can be generated. Embedding the tissue blocks with wax or celloidin makes it very difficult to remove all of it completely at the later stages before IHC. Incomplete removal of these embedding materials introduces staining artefacts. Significant loss of details, drying artefacts, opacity artefacts caused by imperfect dehydration, changes in tissue and nuclear morphology by enlargement of cells and nuclei during drying, uneven staining due to slide mounted staining techniques, incomplete fixation in PETS creating zonal fixation, poor and uneven penetration of the fixative causes inconsistent results across sections. Tissue folds and wrinkles can be introduced during tissue retrieval for frozen sections and as mechanical damages for PETS. Cracks and holes, as freezing artefacts, tissue compression and distortion are other artefacts that may be introduced during tissue slice acquisition.

To mitigate these technical limitations and high artefact count with paraffin embedded tissue slice acquisition technique, generating thick free floating tissue slices using a freezing microtome (-18°C) is a suitable alternative. 50µm thick free floating tissue slices provide significant advantages over the other two methods – even staining, appropriate tissue thickness for applying standard stereological analysis, reduced chemical pre-processing before tissue staining with IHC preserving antigenicity and the possible application of antigen-retrieval techniques for unmasking sensitive epitopes. But this technique also possesses the potential to generate significant tissue artefacts in terms of freezing artefacts (cracks, holes), tissue consistency (thin/thick sections within the same section), shearing artefacts and compression artefacts due to the formation of ice crystals.

An agarose embedding protocol was developed and adopted to eliminate all these artefacts. 4% low-melting agarose was used to create a cast within which the brainstem block was embedded. Once this cast was created, it was then submerged in 30% sucrose solution to replace all the excess water for a period of 48 hours. This brainstem block casting protocol eliminated the artefacts that were generated otherwise with a block of similar dimensions when using a freezing microtome.

3.4 Experimental Design – Heating water bath setup

The 50 µm thick tissue slices, large brainstem tissue block and small brainstem tissue block were subjected to the heat-induced antigen retrieval technique with the help of a heating water bath.

All tissue sizes were submerged in the specific retrieval buffer overnight and stored at 4°C before being subjected to the HIER process the following day. Prior to the HIER process, the tissues were transferred into new retrieval buffer kept at room temperature. The large and small tissue blocks were transferred into a zip-lock bag filled with the retrieval buffer, while the 50 µm thick tissue slices were transferred into 6-well cell culture plates filled with the retrieval buffer (5mL/per well) and a thin paraffin sheet was used to cover all the wells. This was performed to prevent the solution from evaporating. The lid was then placed, and the plate submerged in the heating water bath.

3.5 Immunohistochemistry

Free floating 50µm thick sections were used for immunohistochemistry (IHC). First, the sections were rinsed in 1x PBS several times to remove the antifreeze while on a shaker. This was followed by treating the sections with 1.5% hydrogen peroxide (H₂O₂) in 1x PBS for 10 mins at room temperature (RT) to quench the endogenous peroxidase activity. Then, the sections were rinsed thrice with 1x PBS and then incubated in a blocking solution. The blocking solution varied based on the antibody used for IHC. In general, the blocking solution was composed of 5% BSA (Bovine Serum Albumin) and 0.3% 1x-Triton X-100 in PBS. The sections were incubated for a period of 2 hours at RT. The sections were then removed from the blocking solution and incubated in the primary antibody solution. The primary antibody solution was prepared by mixing 3% BSA and 0.1% 1x-Triton X-100 with the required concentration of the primary antibody. The sections were then first incubated at RT for 2 hours, followed by an incubation at 4°C for 24 - 48 hours, followed by a 2-hour RT incubation period. Sections were then rinsed multiple times in 1x PBS to remove the excess primary Ab, which was followed by a secondary antibody incubation. The sections were incubated for 2 hours at RT in the secondary antibody mix containing the appropriate secondary Ab in a 3% BSA and 0.1% 1x-Triton X-100 mixture. This immunohistochemical signal was amplified using a (Horseradish Peroxidase) HRP tagged ABC (Avidin-Biotin Complex) system. This amplification required an incubation period of 2 hours at RT which was preceded by rinsing the sections thrice with 1x PBS. After incubating the sections in the ABC mixture, the sections were washed twice with 1x PBS and then once with 0.05M tris buffer. The sections were then incubated in the DAB (3,3'-diaminobenzidine) mixture at RT for 10-15 mins with visual monitoring of the signal development. The DAB mixture is composed of 0.025% DAB as the chromogenic substrate in a 0.05M tris buffer (pH 7.6), 1% imidazole and 0.006% H₂O₂. Following signal detection, the sections were thoroughly rinsed with 0.05M tris buffer first and then with 1x PBS to stop the reaction and rid the sections of any excess DAB.

The basic standard immunohistochemistry protocol for staining human brain tissue previously established in laboratory with DAB and Nickel-DAB is as follows.

PARAMETERS	VARIANTS	Incubation Times	Solution Used
Quenching	1.5% H ₂ O ₂	20 mins @ RT	0.1M PBS

Blocking	0.3% Triton	5% BSA	1 hr @ RT		0.1M PBS
Primary Antibody	0.1% Triton	2% BSA	Overnight (18 hours @ 4°C)		0.1M PBS
Secondary Antibody	0.1% Triton	2% BSA	1 hr @ RT		0.1M PBS
ABC	0.1% Triton	2% BSA	1 hr @ RT		0.1M PBS
Revealing Step	DAB	Ni-DAB	15 mins	9 mins	0.05M TBS

To determine the optimal conditions for pronounced activity by the respective antibodies, different parameters were titrated for, till the ideal combination was achieved. The following table represents in brief the overall titration scheme.

PARAMETERS	VARIANTS (BLOCKING STEP)						
Treatment Solution	0.1M PBS	0.05 M TBS					
Triton Concentration	0.0025%	0.005%	0.05%	0.1%	0.2%	0.3%	0.5%
BSA Concentration	5%	10%					
Anti-Secondary Serum Concentration	3%	5%	10%				
Incubation Times	1 hr @ RT	1 hr 30 mins @ RT	2 hrs @ RT				

PARAMETERS	VARIANTS (PRIMARY ANTIBODY)
-------------------	------------------------------------

Treatment Solution	0.1M PBS	0.05 M TBS					
Triton Concentration	0.0025%	0.005%	0.05%	0.1%	0.2%	0.3%	0.5%
BSA Concentration	2%	3%	5%	10%			
Anti-Secondary Serum Concentration	2%	3%	5%	10%			
Incubation Times	Overnight (18 hours @ 4°C)	24 hrs @ 4°C	48 hrs @ 4°C	72 hrs @ 4°C	1 hr @ RT + 22 hrs @ 4°C + 1 hr @ RT	1 hr @ RT + 46 hrs @ 4°C + 1 hr @ RT	2 hrs @ RT + 44 hrs @ 4°C + 2 hrs @ RT
Primary Antibody Concentration	Start with the vendor's recommended concentration and vary based on the results. Usually 1:1000 was taken as a good starting point. Final concentration – anti-TPH2 (1:5000) and anti-SERT (IS) (1:5000).						

PARAMETERS	VARIANTS (SECONDARY ANTIBODY)						
Treatment Solution	Use the solution that the primary antibody was made in.						
Triton Concentration	0.0025%	0.005%	0.05%	0.1%	0.2%	0.3%	
BSA Concentration	2%	3%	5%	10%			

Anti-Secondary Serum Concentration	2%	3%	5%	10%			
Incubation Times	1 hr @ RT	1 hr 30 mins @ RT	2 hrs @ RT				
Secondary Antibody Concentration	The standard established laboratory concentration of 1:250 was used for all antibodies.						

PARAMETERS	VARIANTS (ABC)						
Treatment Solution	Use the solution that the primary antibody was made in.						
Triton Concentration	0.0025%	0.005%	0.05%	0.1%	0.2%	0.3%	
BSA Concentration	2%	3%	5%				
Anti-Secondary Serum Concentration	2%	3%	5%				
Incubation Times	1 hr @ RT	1 hr 30 mins @ RT	2 hrs @ RT				
ABC Concentration	The standard established laboratory concentration of 1:100 of Reagent A and Reagent B of the ABC Universal Kit was used for all antibodies.						

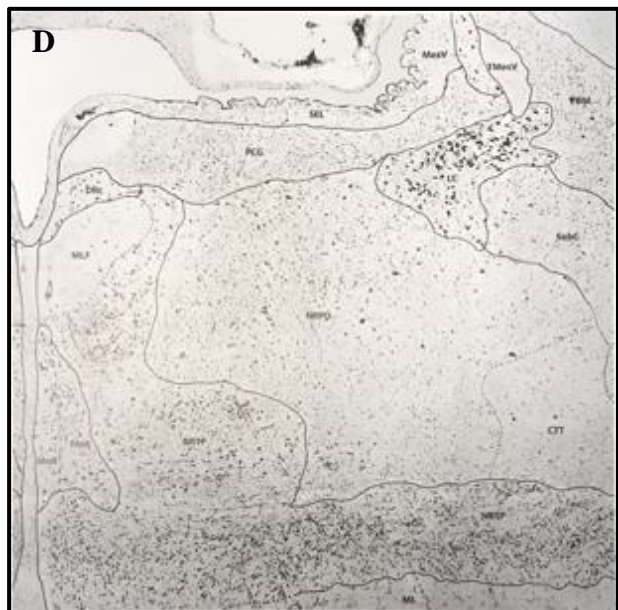
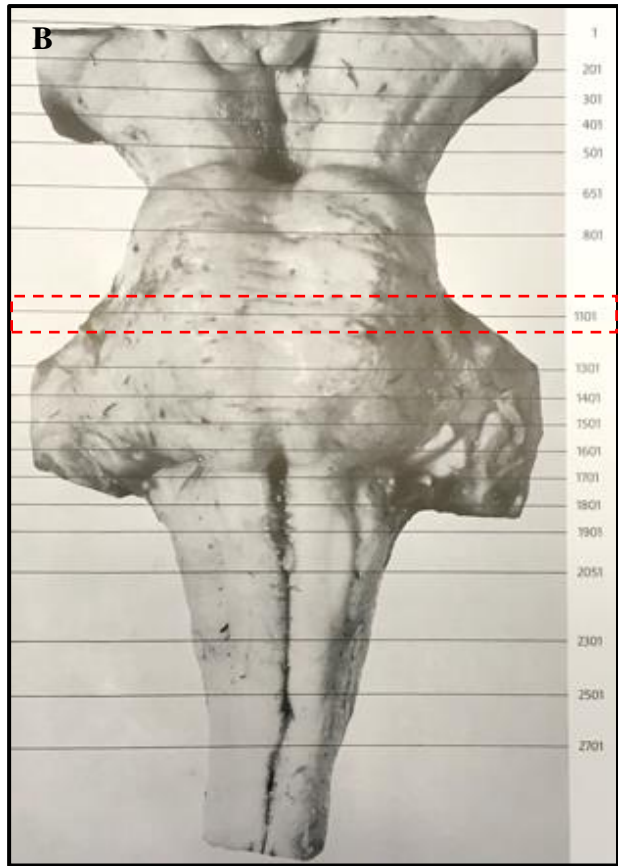
PARAMETERS	VARIANTS

Treatment Solution	Use the solution that the primary antibody was made in.
Incubation Times (DAB)	Sections are tested for a range starting from 10 to 15 mins and the most optimal time is recorded to be used for successive staining. Timings may vary across antibodies for similar tissue size and architecture.
Incubation Times (Ni-DAB)	Sections are tested for a range starting from 5 to 9 mins and the most optimal time is recorded to be used for successive staining. Timings may vary across antibodies for similar tissue size and architecture.

3.6 Digitization of Histological Sections

To acquire detailed chemo- and cyto-architectonic profiles of the sections, a semi-automated, whole slide scanning technique was adopted. The sections were scanned at a resolution of 0.64 μ m/pixel using a 10x and 5x objective with a numerical aperture of 0.3. AxioImager Z2 Vario (Carl Zeiss, Germany) with a motorized specimen stage customized for large slide imaging coupled to an EC Plan NeoFluar 10x objective was used for scanning. Images were taken via the Stereoinvestigator (MBF Biosciences, USA) software.

CHAPTER 4: RESULTS



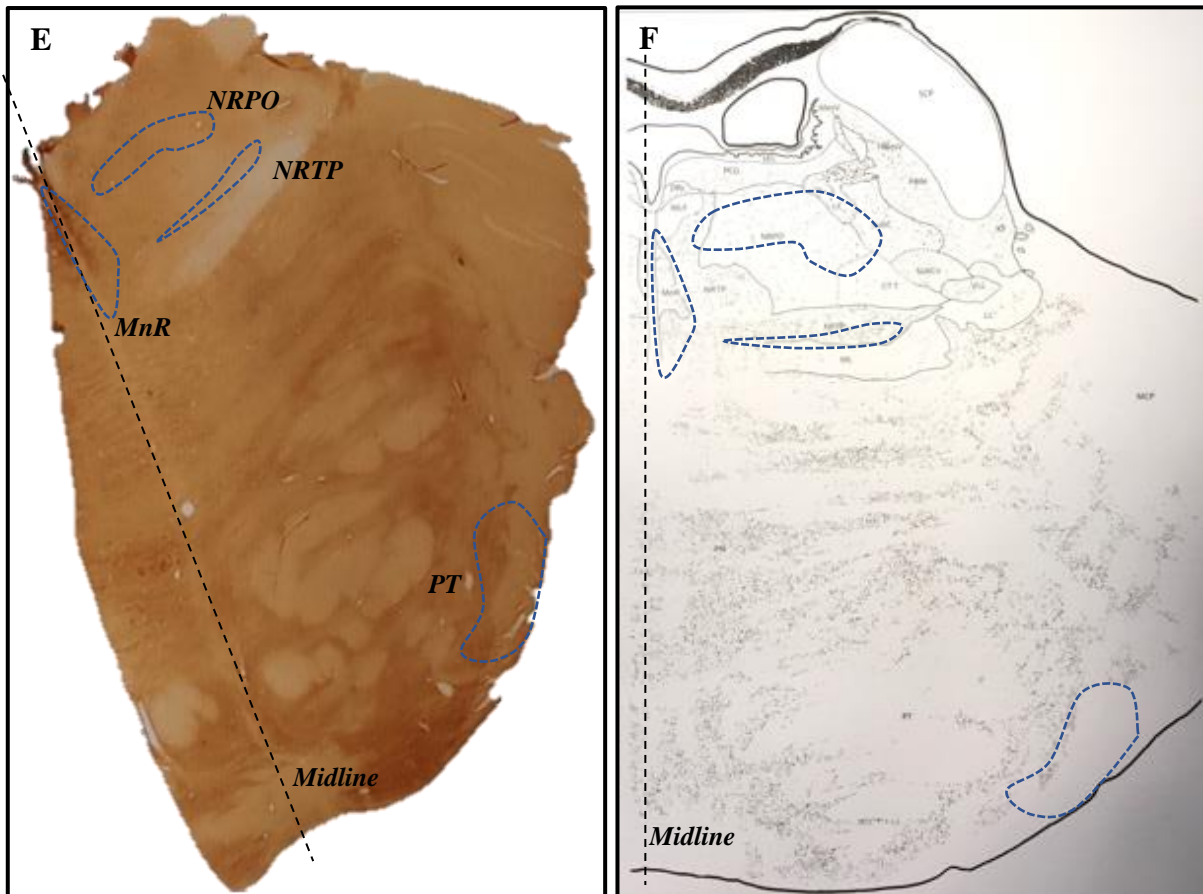


Figure 2: Reference Image 1: Tissue sectioned at the level of Pons. (A) Representative image sectioned at the level of the pontine nuclei. (B) Corresponding level shown according to Olszewski and Baxter's Human Brainstem Atlas. (C) A semi-schematic representation of the cross-section marked in red in (B). (D) A 40x magnification of the semi-schematic representation of the cross-section marked in red in (B). (E-F) According to Olszewski and Baxter's Human Brainstem Atlas regions corresponding to the median raphe (MnR), Paramedian raphe nucleus (PMR), the nucleus reticularis tegmenti pontis (NRTP), the nucleus reticularis pontis oralis (NRPO) and the pyramidal tract (PT) are outlined in blue. These four regions are represented throughout the study for to account for the variability in staining and antigen retrieval profiles using different methods. (B, C, D, F) Adapted from Büttner-Ennever, J. A., & Horn, A. K. (Eds.). (2014). Olszewski and Baxter's Cytoarchitecture of the human brainstem. Basel: Karger.

shown according to Olszewski and Baxter's Human Brainstem Atlas. (C-D) According to Olszewski and Baxter's Human Brainstem Atlas, regions corresponding to the nucleus raphe magnus (RMg), gigantocellular nucleus (Gi), the ventral laminae of the principal olive (VL) and the pyramidal tract (PT) are outlined in blue. These four regions are represented throughout the study for to account for the variability in staining and antigen retrieval profiles using different methods. (B, D) Adapted from Büttner-Ennever, J. A., & Horn, A. K. (Eds.). (2014). Olszewski and Baxter's Cytoarchitecture of the human brainstem. Basel: Karger.

4.1 Compare and optimise the various heat-induced antigen retrieval techniques & protocols to increase the efficiency of standard IHC techniques.

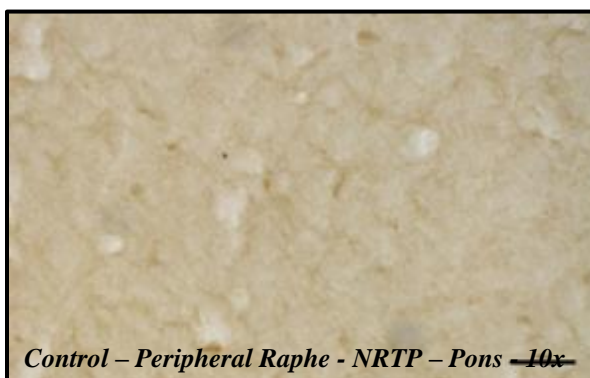
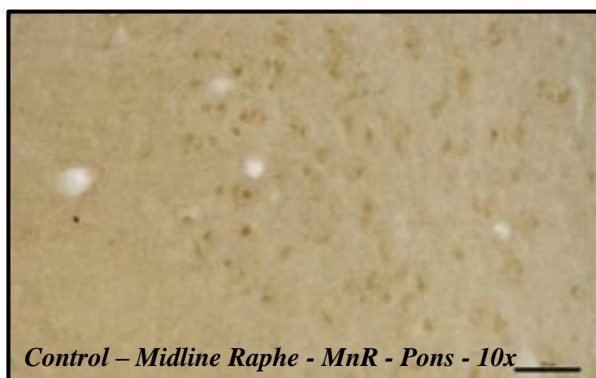
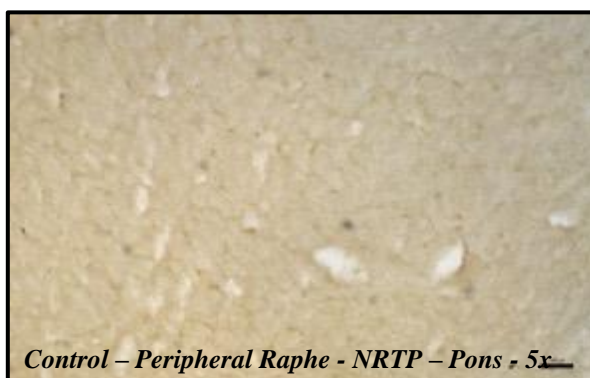
The following describes the standardisation and determination of the best antigen retrieval protocol for the human brainstem tissue, for the serotonergic markers – TPH2 & SERT - for the parameters of pH, time, and type of buffer for tissue slices. A comparative study of the efficacy of antigen retrieval on tissue blocks (large and small) and tissue slices was performed.

(A) Determination of the efficacy of HIER protocol on tissue blocks and free-floating sections

To determine the efficacy of HIER on tissue blocks vs free floating tissue, the 0.1M sodium citrate buffer (pH 6.0) was used. In one group, large and small brainstem blocks were subjected to antigen retrieval whereas in the other, 50µm thick tissue slices were subjected to antigen retrieval. As antigen retrieval is routinely performed on slide-mounted sections and not on free-floating sections, a protocol to successfully perform antigen retrieval on tissue slices without damaging the tissue quality was developed.

Specimen	Buffer	pH	Time-Temperature	Antibodies Tested
Brainstem Tissue (B2) – Large	0.1M Sodium Citrate	6.0	20 mins @ 90°C	TPH2, SERT (IS)

Block (3x2x5 cm ³ approx.)				
Brainstem Tissue (B1) – Small Block (3x2x2 cm ³ approx.)	0.1M Sodium Citrate	6.0	20 mins @ 90°C	TPH2, SERT (IS)
Brainstem Tissue (B1) – Slice	0.1M Sodium Citrate	6.0	20 mins @ 90°C	TPH2, SERT (IS)
CONTROL: Brainstem Tissue Slice (B1)	NA	NA	NA	TPH2, SERT (IS)
CONTROL: Brainstem Tissue Slice (B1)	NA	NA	NA	NA



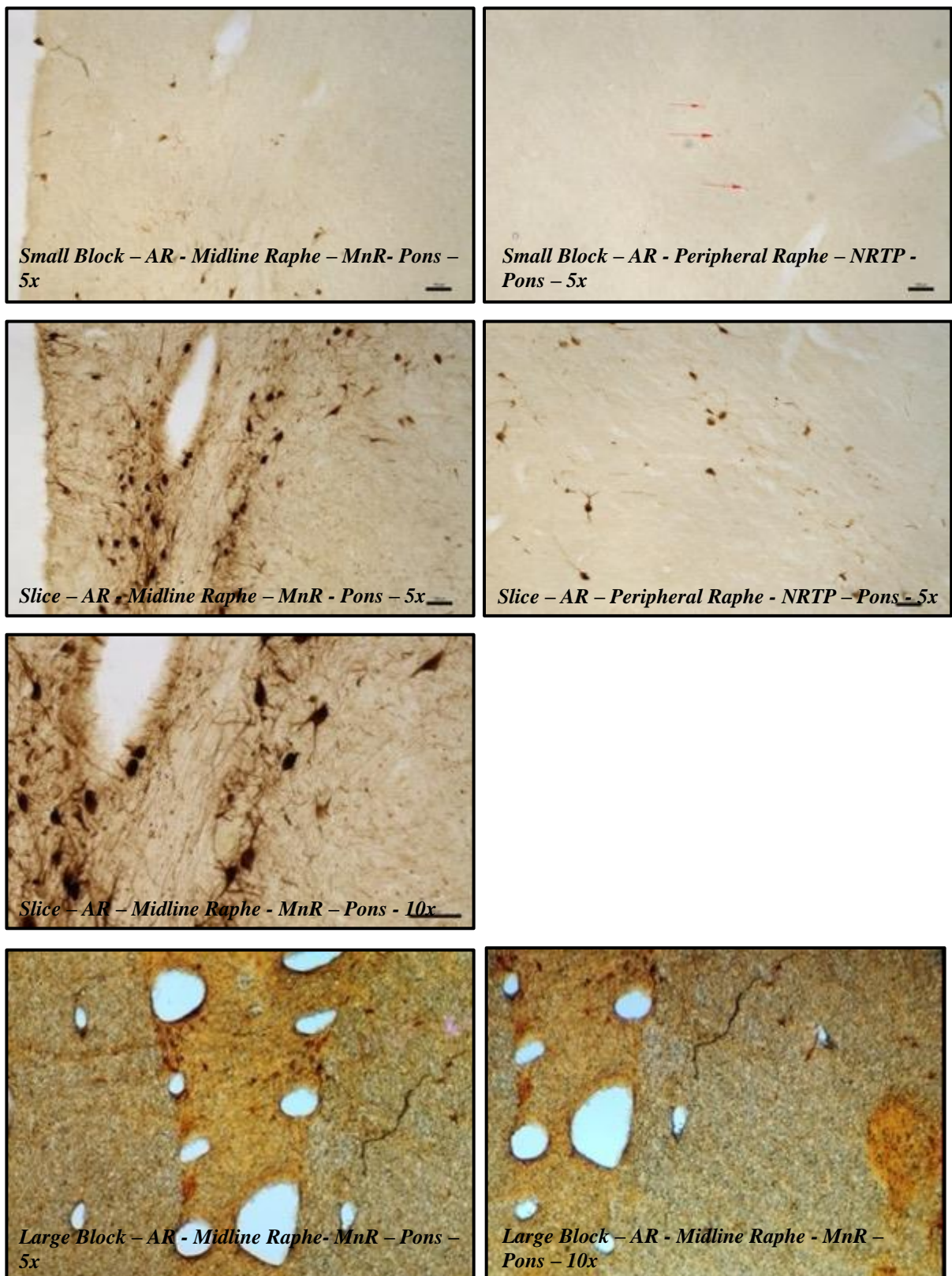


Figure 4: Determination of the efficacy of HIER protocol on tissue blocks (large and small) and free-floating sections on staining intensity and definition. Anti-Tryptophan Hydroxylase 2 Ab – 1/5000 – 0.1M Sodium Citrate @ pH 6.0; 90°C for 20 mins was the antibody used for the test. Performing the antigen retrieval on 50µm thick tissue slices generated the most

consistent and uniform staining with anti-TPH2 antibody under standard conditions. The small and large blocks allowed for insufficient penetration of the antigen retrieval buffer causing variable unmasking. The tissue temperature for the internal regions potentially might not have reached the target 90°C when incubated for a duration of 20 mins, while keeping the solution longer at such high temperatures would damage the external tissue surface. A combination of poor antigen retrieval buffer penetration and an inadequately raised internal temperature might contribute to the poor and inconsistent staining of serotonin cells with anti-TPH2 with the presence of high background noise. Regions corresponding to the median raphe (MnR), Paramedian raphe nucleus (PMR), the nucleus reticularis tegmenti pontis (NRTP) and the nucleus reticularis pontis oralis (NRPO) according to the Olszewski and Baxter's Human Brainstem Atlas are represented here.

Using the above experimental setup, I could observe that performing the antigen retrieval on 50µm thick tissue slices was the most optimal as uniform and sufficient penetration of the retrieval buffer into the slices was achieved, leading to uniform unmasking of the target epitopes. The small and large blocks allowed for insufficient penetration of the antigen retrieval buffer causing variable unmasking. The tissue temperature for the internal regions potentially might not have reached the target 90°C when incubated for a duration 20 mins, while keeping the solution longer at such high temperatures would damage the external tissue surface. A combination of poor antigen retrieval buffer penetration and an inadequately raised internal temperature might contribute to the poor and inconsistent staining of serotonin cells with anti-TPH2 with the presence of higher background noise.

<i>Buffer Type(pH)/Temperature</i>	<i>Sodium Citrate (Wrinkles) (90°C)</i>	<i>Sodium Citrate (Tears) (90°C)</i>	<i>Distilled Water (RT) (No AR)</i>
<i>Large Block tissue</i>	-	-	-
<i>Small Block tissue</i>	-	-	-
<i>50µm thin tissue slice</i>	++	-	-

Table 2: Determination of the effect of buffer & pH and temperature on tissue structural integrity when AR is applied to tissue slices, very small blocks, and large blocks in introducing folds and wrinkles as artefacts and in increasing the fragility of the sections leading to the possibility of microtears. 0.1M Sodium citrate buffer at neutral pH (pH 6.0 was

used as test carrier immersion buffer. Distilled water used as the control to test for the effect of temperature on the tissue slices. Wrinkles are defined as the folding up of the tissue slice, due to one of the factors causing tissue shrinkage and tears, as an outcome of the fragility introduced by the specific antigen retrieval treatments. Wrinkles are rated on a scale of (-, +, ++, +++) representing absent, low (1 wrinkle), medium (2-4 wrinkles) or high (5+ wrinkles) respectively. Tears are rated on a scale of (-, +, ++, +++) representing absent, low (1 microtear at the edge), medium (2-4 microtears at the edges) or high (complete clear tear within the section) respectively.

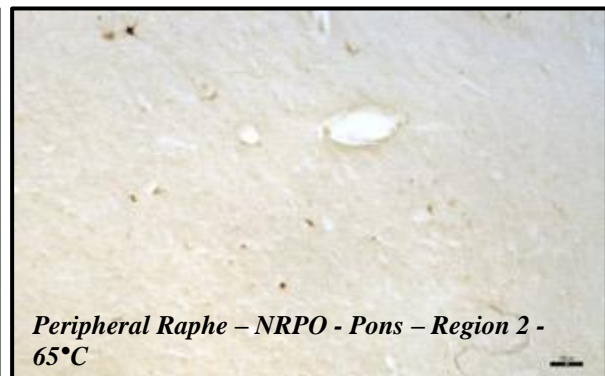
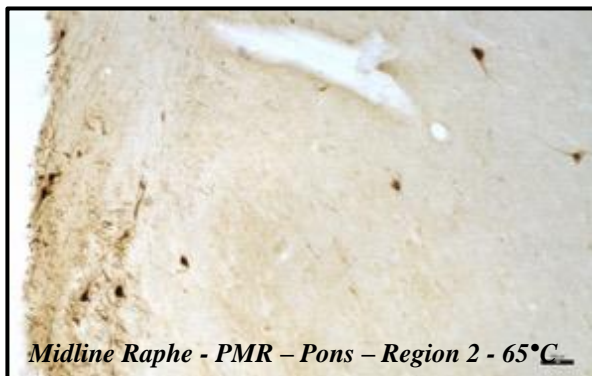
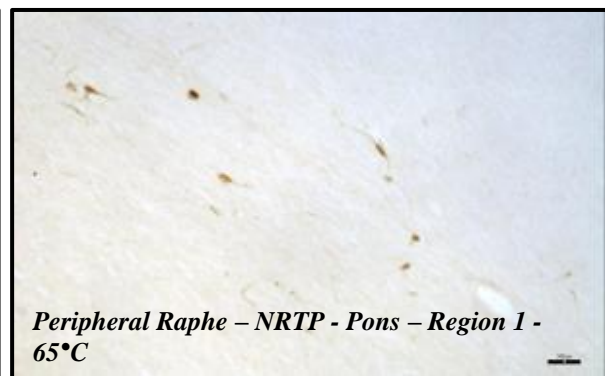
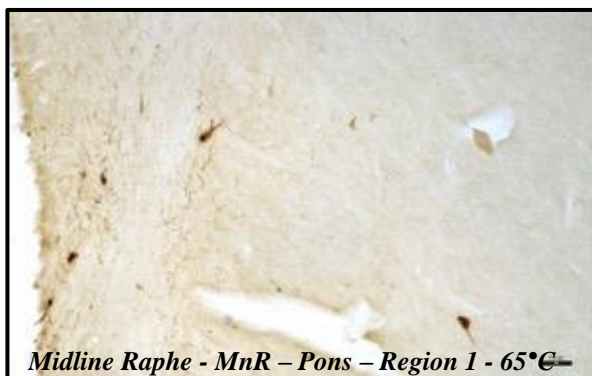
Tissue thickness seemed to slightly affect the introduction of wrinkles during mounting. Antigen retrieved 50µm thick tissue slices although were not any more difficult to mount when compared to the HIER applied small and large tissue blocks, they did carry a tendency to fold over and caused a few wrinkles appear. The tissue slices generated from tissue blocks subjected to HIER did not show any form of structural/tissue integrity compromise or introduction of folds.

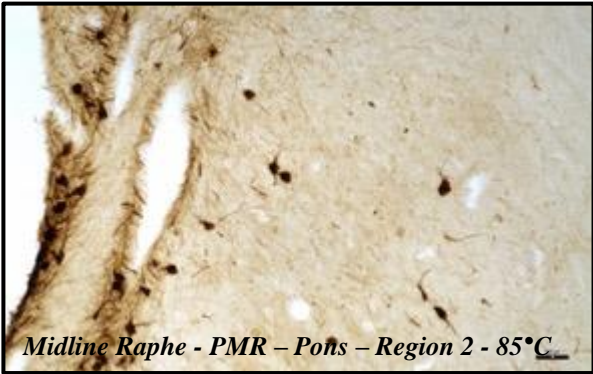
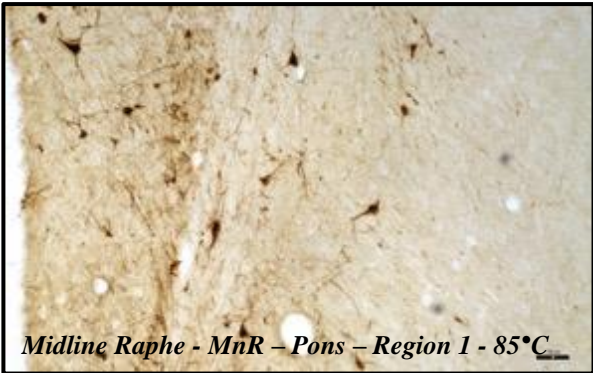
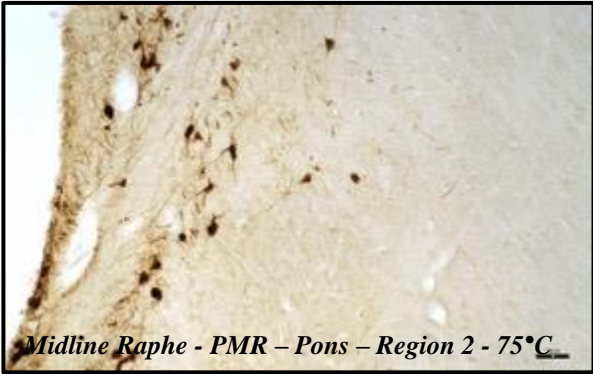
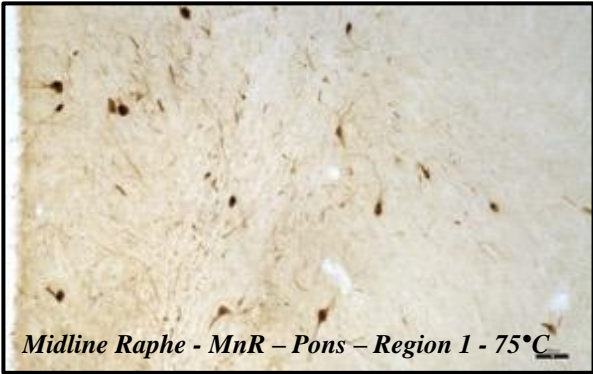
(B) *Effect of temperature on HIER on staining intensity, definition, and tissue structural integrity*

To determine the effect of a range of temperatures on its epitope unmasking capabilities, double distilled water was used as the carrier buffer. The following experimental setup was tested on 50 µm thick brainstem sections at the temperature ranges of 65°C – 95°C in increments of 10°C for 20 mins in a boiling water bath. The control tissue was kept at room temperature for an incubation period of 20 mins in double distilled water.

Specimen	Buffer	Time-Temperature	Antibodies Tested
Brainstem Tissue (B1) – Slice	Double Distilled Water	20 mins @ 95°C	TPH2, SERT (IS)
Brainstem Tissue (B1) – Slice	Double Distilled Water	20 mins @ 85°C	

Brainstem Tissue (B1) – Slice	Double Distilled Water	20 mins @ 75°C	
Brainstem Tissue (B1) – Slice	Double Distilled Water	20 mins @ 65°C	
CONTROL: Brainstem Tissue (B1) – Slice	Double Distilled Water	No Heat Applied/Kept at Room Temperature for 20 mins	





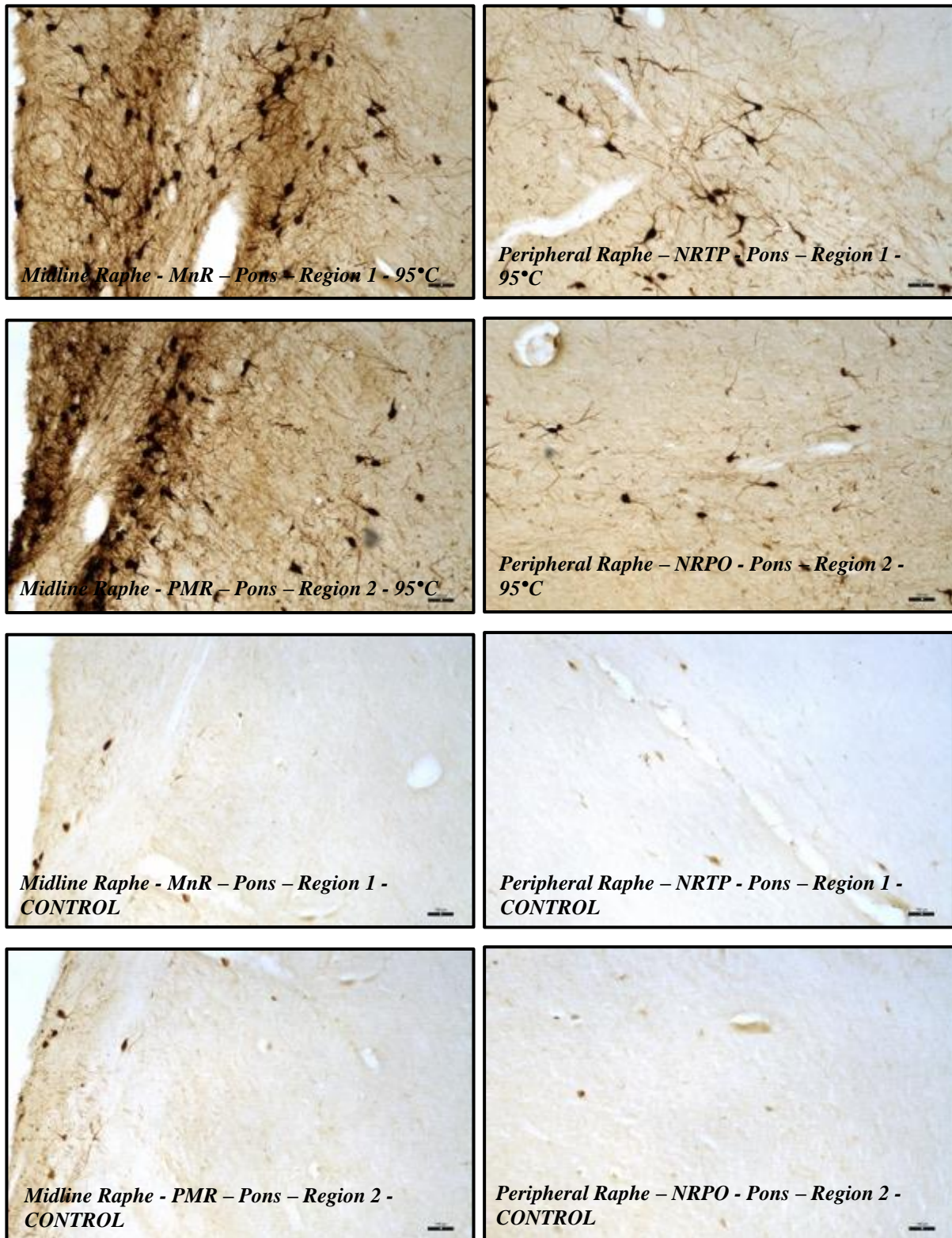


Figure 5: *Effect of temperature on HIER on staining intensity, definition, of serotonergic cell bodies in the midline and lateral serotonin cell groups at the level of DRN. The cells are stained for TPH2 antibody (1:5000). Double distilled water is used as the carrier/immersion solution. With the increase in the temperature, a significant increase in the visibility and staining intensity of the serotonergic cells is observed. The effect of the increase in temperature*

for staining intensity is more drastic for the peripheral/lateral serotonergic neurons when compared to the midline neurons. An increase in the visualisation of the proximal dendrite distribution of the same is also observed. But increased background noise can also be seen with the increase in the temperature which needs to be reduced by using alternative measures. Regions corresponding to the median raphe (MnR), paramedian raphe nucleus (PMR), the nucleus reticularis tegmenti pontis (NRTP) and the nucleus reticularis pontis oralis (NRPO) according to the Olszweski and Baxter's Human Brainstem Atlas are represented here.

Using the above experimental setup, a direct correlation between temperature and serotonin cellular staining can be seen. With increasing temperatures, increased staining intensity and cellular definition was achieved. A significant increase in background staining could also be observed with the increase in the temperature. The highest staining intensity was achieved with the application of heat at the temperature of 95°C. Although lower cellular staining intensity was observed at 85°C comparatively, it too provided a clear cellular definition with good staining. But this temperature produced less background staining as compared to the tissue subjected to 95°C heat.

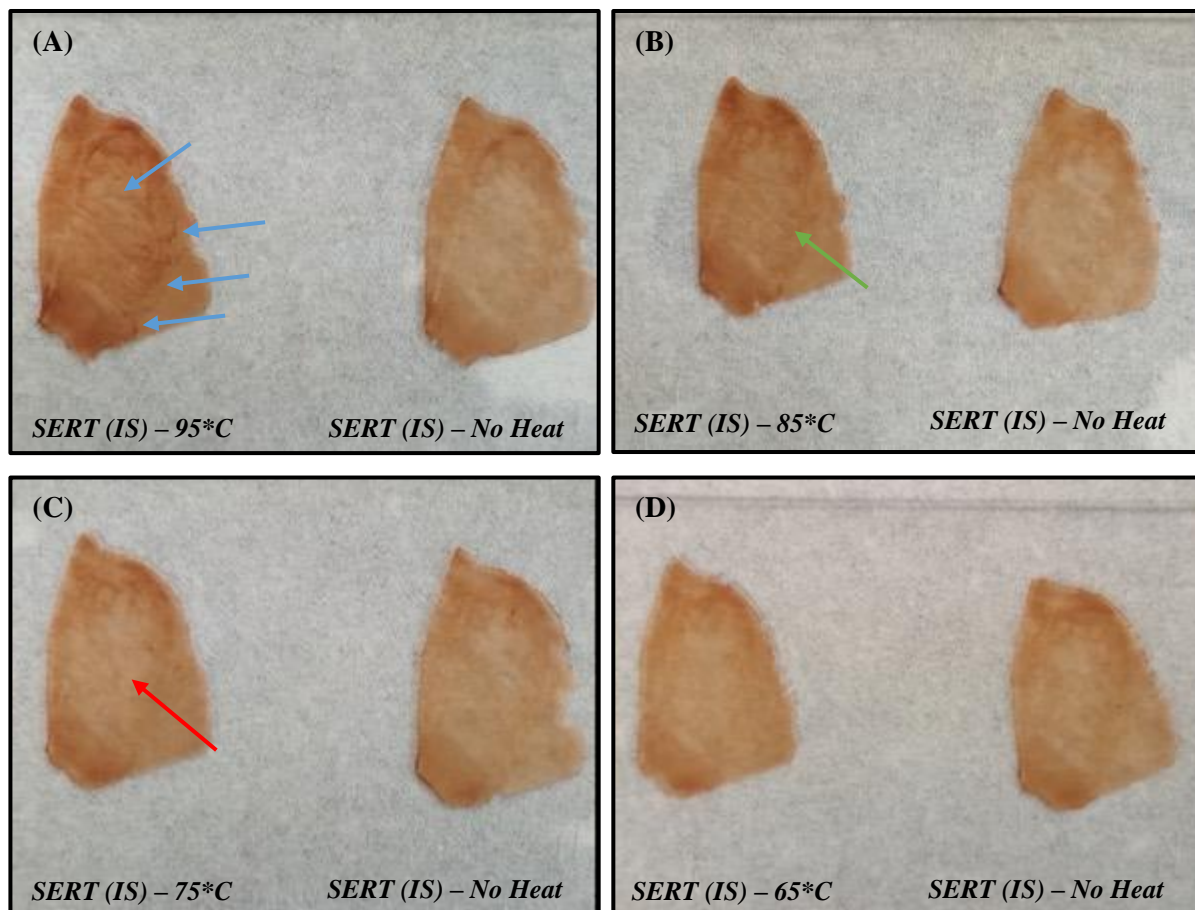


Figure 6: Effect of buffer & pH and temperature in introducing folds and wrinkles as artefacts and in increasing the fragility of the sections leading to the possibility of microtears. The tissue slices represented here were tested for using the anti-SERT (Immunostar – 1:5000) antibody in double distilled water. (A) The representative images here show the increase in folds and wrinkles due to exposure to higher temperatures (95°C). (B-C) A very small wrinkle occurred during mounting due to the folding up of the tissue. (D) No wrinkles were seen during mounting. With increasing temperatures, and stronger buffers (higher pH), the tissue fragility increases, causing the tissue to fold over. Using lower temperatures of around 85°C seems to provide the benefits of the improved staining without introducing any significant wrinkles, folds or compromising the tissue structural integrity.

<i>Type/Temperature</i>	<i>Buffer 65°C</i>	<i>75°C</i>	<i>85°C</i>	<i>95°C</i>	<i>RT</i>
<i>Distilled Water (Wrinkles)</i>	-	+	+	++	-
<i>Distilled Water (Tears)</i>	-	-	-	+	-

Table 3: Determination of the effect of temperature in introducing folds and wrinkles as artefacts and in increasing the fragility of the sections leading to the possibility of microtears for SERT-IS (1:5000). Double distilled water was used as test carrier immersion buffer. Distilled water used as the control to test for the effect of temperature on the tissue slices. Wrinkles are defined as the folding up of the tissue slice caused due to one of the factors causing tissue shrinkage and tears are when it occurs as an outcome of the fragility introduced by the specific antigen retrieval treatments. Wrinkles are rated on a scale of (-, +, ++, +++) representing absent, low (1 wrinkle), medium (2-4 wrinkles) or high (5+ wrinkles) respectively. Tears are rated on a scale of (-, +, ++, +++) representing absent, low (1 microtear at the edge), medium (2-4 microtears at the edges) or high (complete clear tear within the section) respectively.

The structural integrity of the tissue is compromised at the temperature of 95°C. Wrinkles and folds are introduced at this temperature, with the tissue carrying a tendency to shrivel. Even though this unwanted secondary effect did not bear much impact on its successful immunohistochemical staining and the subsequent mounting, the folds and the wrinkles would introduce unwanted artefacts if those tissue slices were to be used for a 3D histological reconstruction for the purposes of creating an atlas. Using a lower temperature of 85°C seems

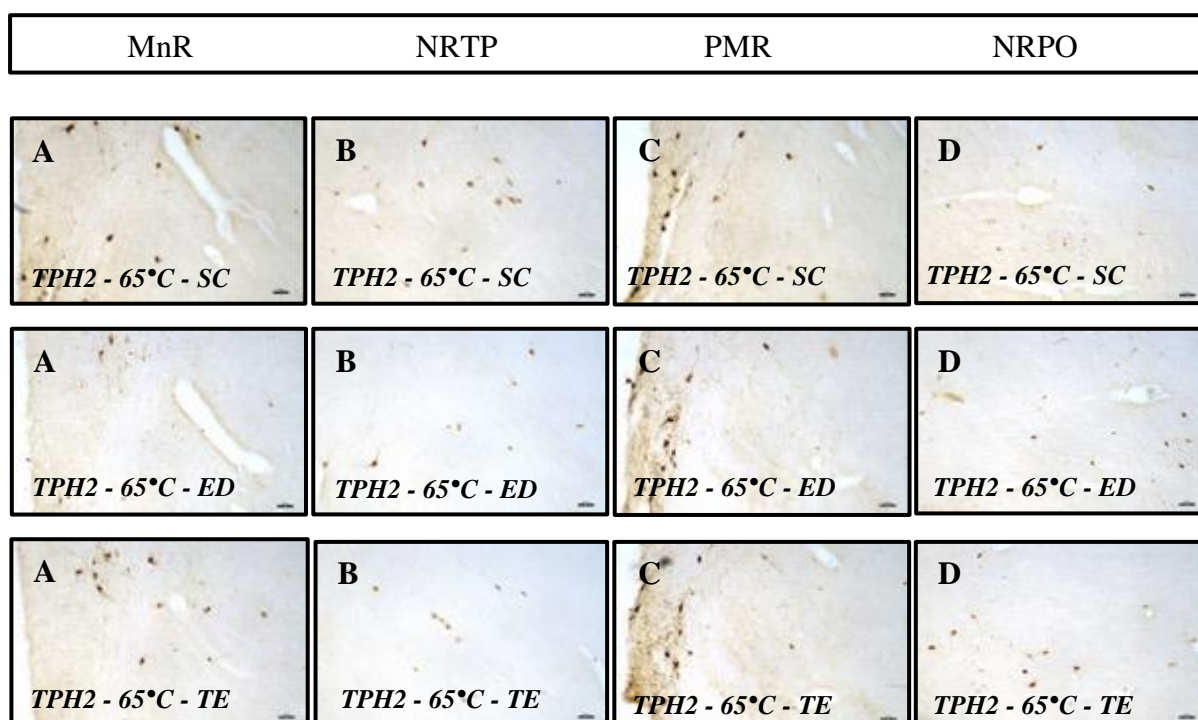
to provide the benefits of improved staining without introducing any significant wrinkles, folds or compromising the tissue structural integrity. On the other hand, if cellular visualisation and quantification is the primary goal, then the higher temperature of 95°C might be more the more suitable parameter.

4.2 Effect of high- and low-pH antigen retrieval buffers on IHC staining and their correlation to temperature

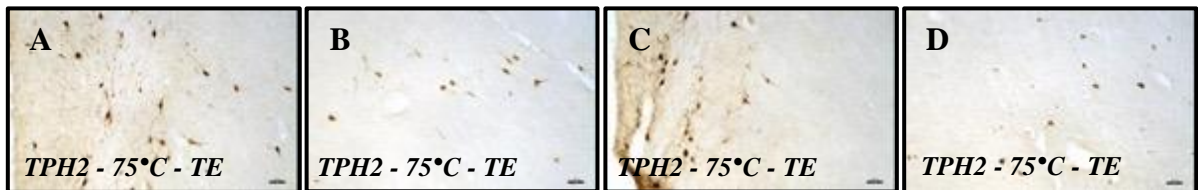
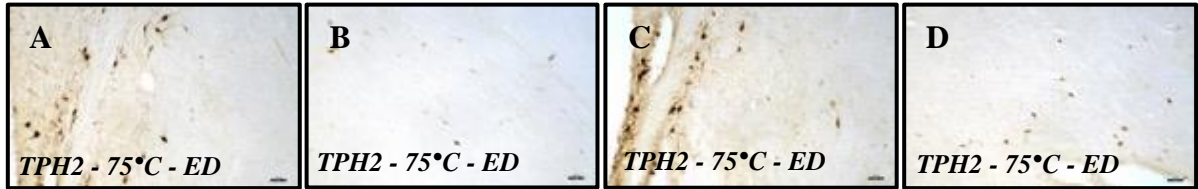
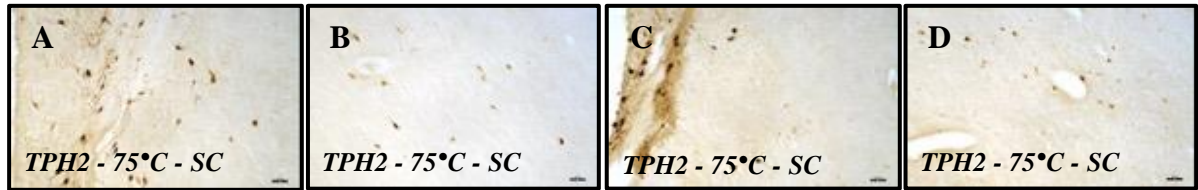
To determine the effect of different antigen retrieval buffers and varying pH (low and high) on its epitope unmasking capabilities, 0.1M Sodium Citrate (pH 6.0), 0.01M EDTA (pH 8.0) and 0.1M Tris-EDTA (pH 9.0) buffers have been tested. These buffers were tested on 50 µm thick brainstem sections for a range of temperatures from 65°C to 95°C in increments of 10°C for 20 mins in a boiling water bath.

Specimen	Buffer	pH	Time-Temperature	Antibodies Tested
Brainstem Tissue Slice (B1)	0.1M Sodium Citrate	6.0	20 mins @ 95°C	TPH2 and SERT (IS)
Brainstem Tissue Slice (B1)	0.1M Sodium Citrate	6.0	20 mins @ 85°C	
Brainstem Tissue Slice (B1)	0.1M Sodium Citrate	6.0	20 mins @ 75°C	
Brainstem Tissue Slice (B1)	0.1M Sodium Citrate	6.0	20 mins @ 65°C	
Brainstem Tissue Slice (B1)	0.01M EDTA	8.0	20 mins @ 95°C	
Brainstem Tissue Slice (B1)	0.01M EDTA	8.0	20 mins @ 85°C	
Brainstem Tissue Slice (B1)	0.01M EDTA	8.0	20 mins @ 75°C	
Brainstem Tissue Slice (B1)	0.01M EDTA	8.0	20 mins @ 75°C	

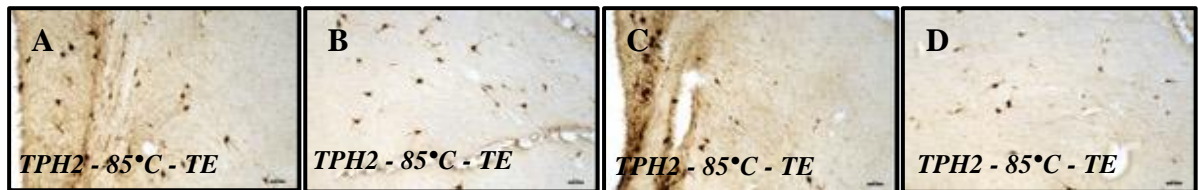
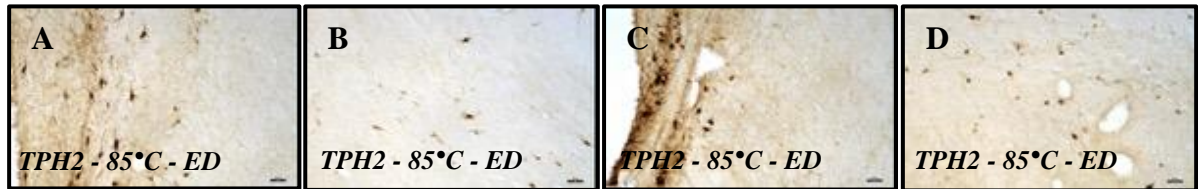
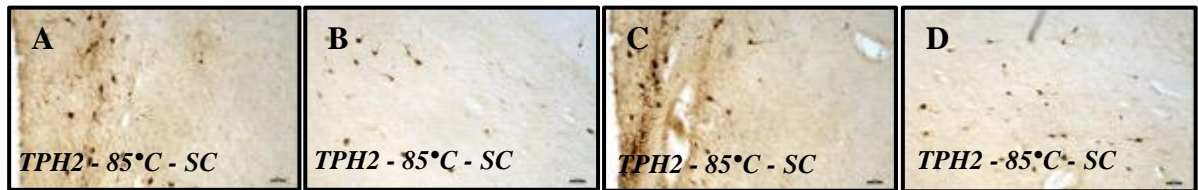
Brainstem Tissue Slice (B1)	0.01M EDTA	8.0	20 mins @ 65°C
Brainstem Tissue Slice (B1)	0.1M Tris-EDTA	9.0	20 mins @ 95°C
Brainstem Tissue Slice (B1)	0.1M Tris-EDTA	9.0	20 mins @ 85°C
Brainstem Tissue Slice (B1)	0.1M Tris-EDTA	9.0	20 mins @ 75°C
Brainstem Tissue Slice (B1)	0.1M Tris-EDTA	9.0	20 mins @ 65°C
CONTROL: Brainstem Tissue Slice (B1)	No buffer used – Distilled Water	7.0	20 mins @ 95°C, 85°C, 75°C and 65°C
CONTROL: Brainstem Tissue Slice (B1)	No buffer used – 0.1M PBS	7.4	NA



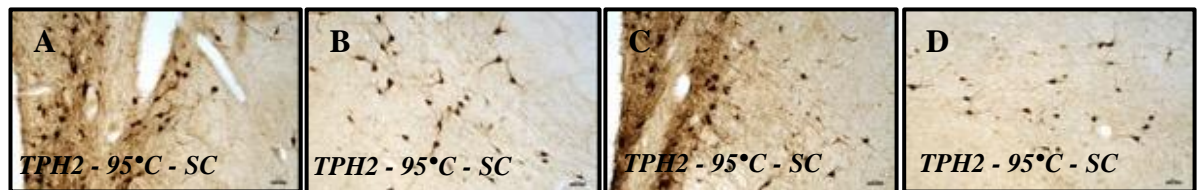
MnR	NRTP	PMR	NRPO
-----	------	-----	------



MnR	NRTP	PMR	NRPO
-----	------	-----	------



MnR	NRTP	PMR	NRPO
-----	------	-----	------



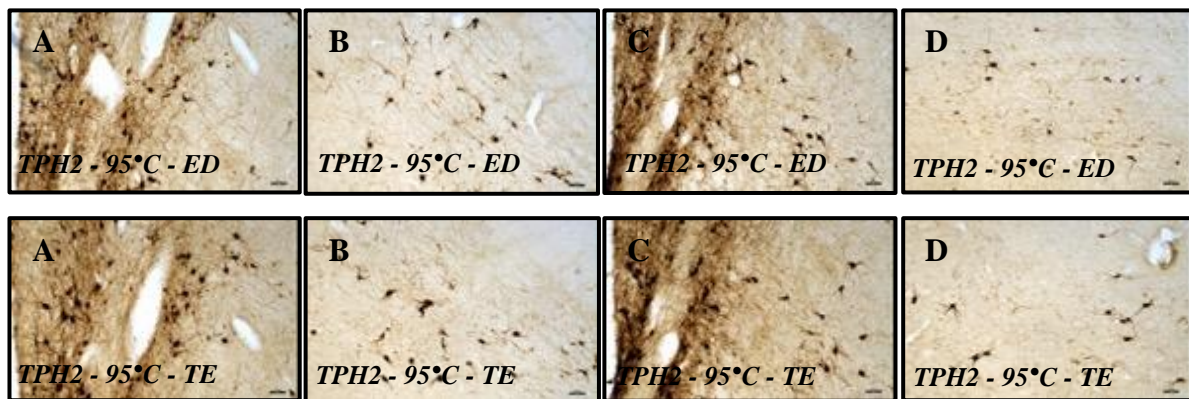


Figure 8: Visualisation of the serotonergic cell bodies – midline and distal/lateral cell bodies, proximal dendritic profiles, observable fiber types and regional projection definitions with the enzyme tryptophan hydroxylase – 2 (Atlas Antibodies – 1:5000) under various AR retrieval parameters of temperature, pH, and buffer type. 0.1M Sodium citrate buffer at neutral pH (pH 6.0) – SC, 0.01M EDTA buffer at high pH (pH 8.0) – ED & low molarity and 0.1M Tris-EDTA buffer at the most basic pH (pH 9.0) – TE were used as test carrier immersion buffers. Distilled water used as the control to test for the effect of temperature on the tissue slices. Columns A, B, C and D correspond to the regions median raphe (MnR), nucleus reticularis tegmenti pontis (NRTP), paramedian raphe nucleus (PMR) and the nucleus reticularis pontis oralis (NRPO) respectively) as per the Olszweski and Baxter’s Human Brainstem Atlas.

	Buffer	65°C	75°C	85°C	95°C	RT
Type(pH)/Temperature						
	Sodium Citrate	+	+	++	+++	+
	EDTA	+	++	++	+++	+
	Tris-EDTA	+	++	+++	+++	+
	Distilled Water	+	+	+	++	+

Table 4: Determination of the most optimal immersion buffer and their performance at various temperatures with regards to staining intensity for TPH2 (1:5000). 0.1M Sodium citrate buffer at neutral pH (pH 6.0), 0.01M EDTA buffer at high pH & low molarity and 0.1M Tris-EDTA buffer at the most basic pH (pH 9.0) were used as test carrier immersion buffers. Distilled water used as the control to test for the effect of temperature on the tissue slices. Staining intensity is defined as how clearly the fibers and cellular profiles are defined from the background at 10x magnification. It is rated on a scale of (+, ++, +++) representing, low intensity, medium intensity, and high intensity respectively.

<i>Buffer</i>	<i>65°C</i>	<i>75°C</i>	<i>85°C</i>	<i>95°C</i>	<i>RT</i>
<i>Sodium Citrate</i>	--	--	-	-	---
<i>EDTA</i>	--	--	--	-	---
<i>Tris-EDTA</i>	--	--	--	--	---
<i>Distilled Water</i>	--	--	-	-	---

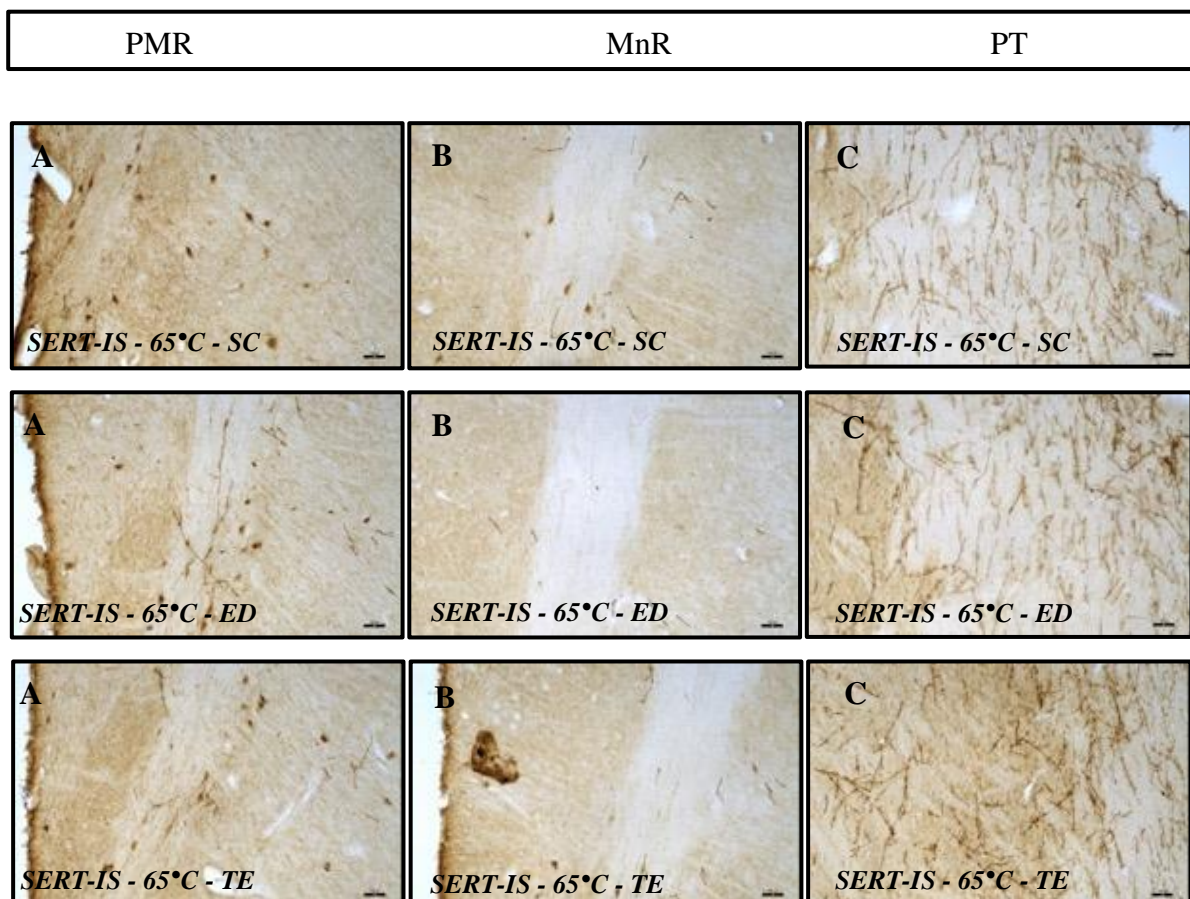
Table 5: Determination of the most optimal immersion buffer and their performance at various temperatures with regards to background staining/noise for TPH2 (1:5000). 0.1M Sodium citrate buffer at neutral pH (pH 6.0), 0.01M EDTA buffer at high pH & low molarity and 0.1M Tris-EDTA buffer at the most basic pH (pH 9.0) were used as test carrier immersion buffers. Distilled water used as the control to test for the effect of temperature on the tissue slices. The background staining is rated on a scale of (-, --, ---) representing, high background noise, medium background noise, and low background noise respectively.

<i>Buffer</i>	<i>65°C</i>	<i>75°C</i>	<i>85°C</i>	<i>95°C</i>	<i>RT</i>
<i>Sodium Citrate (Wrinkles)</i>	-	+	+	++	-
<i>EDTA (Wrinkles)</i>	-	++	++	++	-
<i>Tris-EDTA (Wrinkles)</i>	+	++	+++	+++	-
<i>Distilled Water (Wrinkles)</i>	-	+	++	++	-
<i>Sodium Citrate (Tears)</i>	-	-	-	-	-
<i>EDTA (Tears)</i>	-	-	-	-	-
<i>Tris-EDTA (Tears)</i>	-	-	-	+	-
<i>Distilled Water (Tears)</i>	-	-	-	+	-

Table 6: Determination of the effect of buffer & pH and temperature in introducing folds and wrinkles as artefacts and in increasing the fragility of the sections leading to the possibility of microtears for TPH2 (1:5000). 0.1M Sodium citrate buffer at neutral pH (pH 6.0) – SC, 0.01M EDTA buffer at high pH (pH 8.0) – ED & low molarity and 0.1M Tris-EDTA buffer at the most basic pH (pH 9.0) – TE were used as test carrier immersion buffers. Distilled water used as the control to test for the effect of temperature on the tissue slices. Wrinkles are defined as the folding up of the tissue slice caused due to one of the factors causing tissue

shrinkage and tears are when as an outcome of the fragility introduced by the specific antigen retrieval treatments. Wrinkles are rated on a scale of (-, +, ++, +++) representing absent, low (1 wrinkle), medium (2-4 wrinkles) or high (5+ wrinkles) respectively. Tears are rated on a scale of (-, +, ++, +++) representing absent, low (1 microtear at the edge), medium (2-4 microtears at the edges) or high (complete clear tear within the section) respectively.

0.1M Tris-EDTA (pH 9.0) buffer applied at 85°C for a duration of 20 minutes to 50µm thick slices generated the most optimal and consistent results with the anti-TPH2 antibody. Increased pH in combination with the buffer composition positively impacted cellular staining by reducing the increased background staining that was observed with the increase in the temperature. Even though subjecting the tissue slice to 95°C gave more intense staining, it also came with the drawbacks of tissue folding and wrinkling.



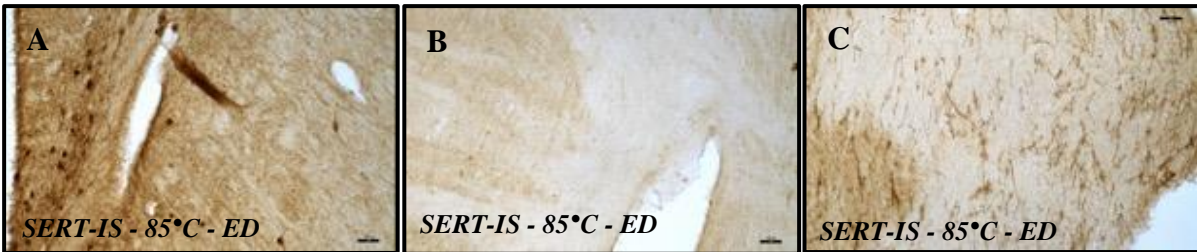


PMR	MnR	PT
-----	-----	----





PMR	MnR	PT
-----	-----	----



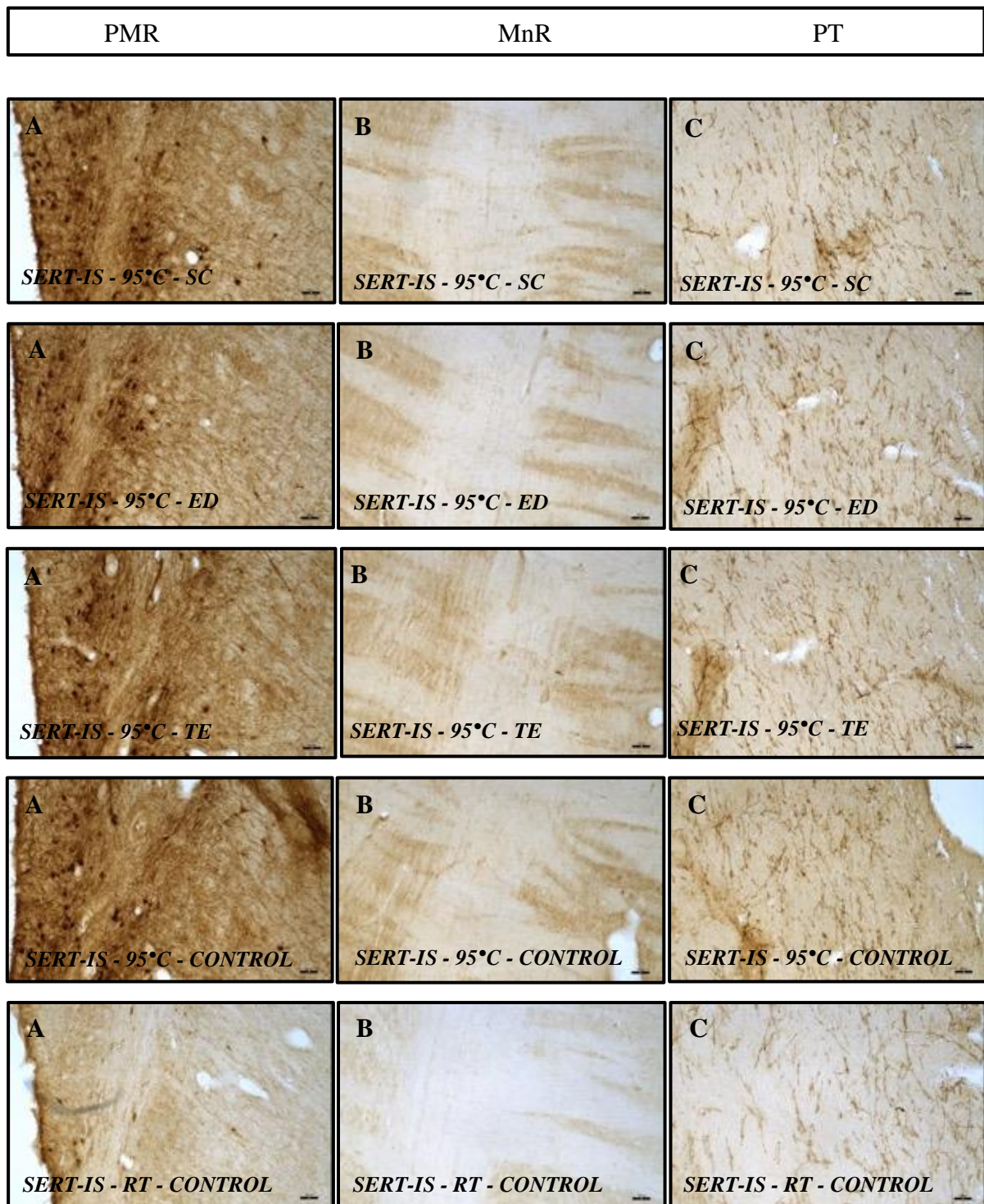


Figure 9: Visualisation of the serotonergic cell bodies, proximal dendritic profiles, fiber types and regional projection definitions with the serotonin transporter (ImmunoStar – 1:5000) under various AR retrieval parameters of temperature, pH, and buffer type. 0.1M Sodium citrate buffer at neutral pH (pH 6.0) – SC, 0.01M EDTA buffer at high pH (pH 8.0) – ED & low molarity and 0.1M Tris-EDTA buffer at the most basic pH (pH 9.0) – TE were used as test carrier immersion buffers. Distilled water used as the control to test for the effect of temperature on the tissue slices. Columns A, B and C correspond to the paramedian raphe

nucleus (PMR), median raphe (MnR) and the pyramidal tract (PT) respectively as per the Olszewski and Baxter's Human Brainstem Atlas.

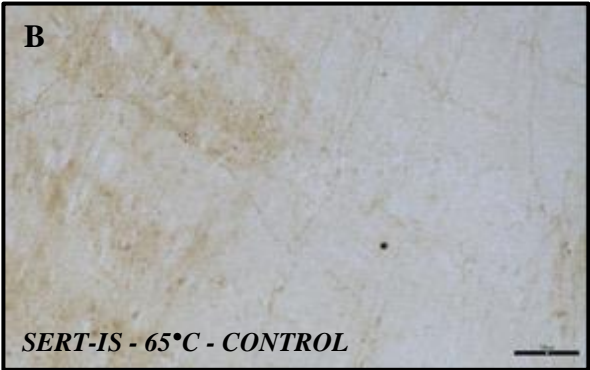
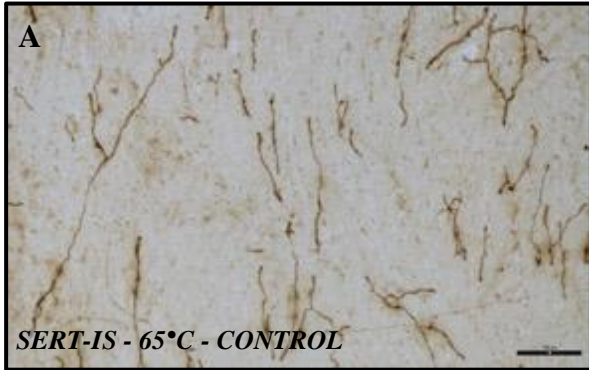
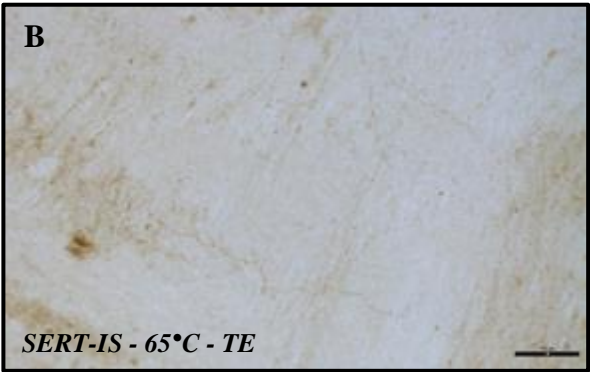
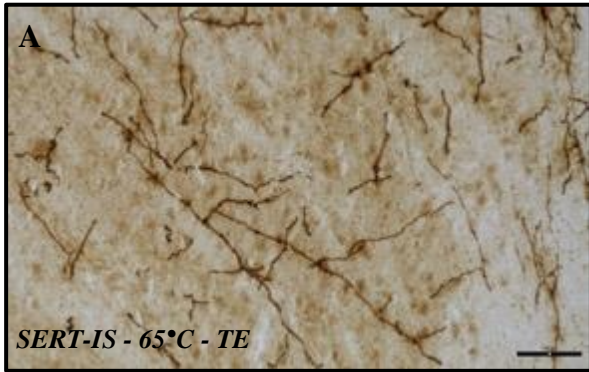
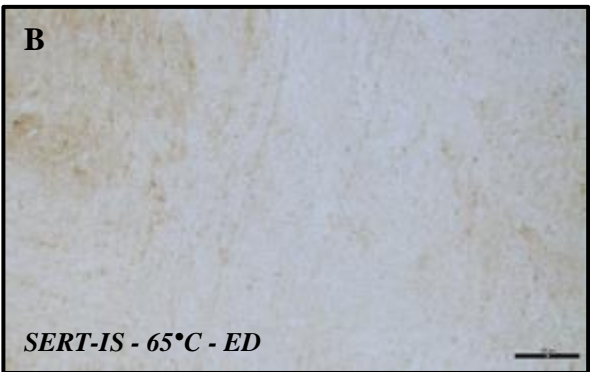
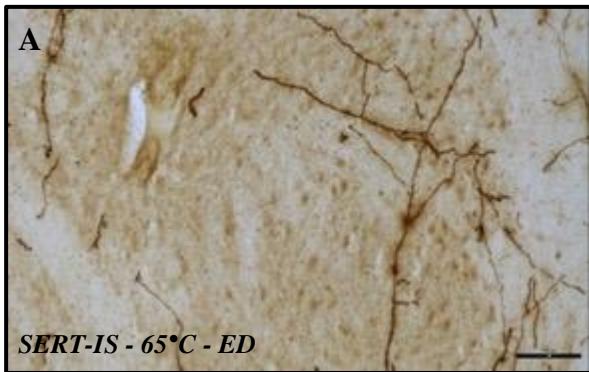
Buffer	65°C	75°C	85°C	95°C	RT
Sodium Citrate	+	+	++	+++	+
EDTA	+	++	+++	+++	+
Tris-EDTA	+	++	++	+++	+
Distilled Water	+	+	++	++	+

Table 7: Determination of the most optimal immersion buffer and their performance at various temperatures with regards to staining intensity for SERT-IS (1:5000). 0.1M Sodium citrate buffer at neutral pH (pH 6.0) – SC, 0.01M EDTA buffer at high pH (pH 8.0) – ED & low molarity and 0.1M Tris-EDTA buffer at the most basic pH (pH 9.0) – TE were used as test carrier immersion buffers. Distilled water used as the control to test for the effect of temperature on the tissue slices. Staining intensity is defined as how clearly the cellular profiles are defined from the background at 10x magnification. It is rated on a scale of (+, ++, +++) representing, low intensity, medium intensity, and high intensity respectively.

Buffer	65°C	75°C	85°C	95°C	RT
Sodium Citrate	--	--	-	-	---
EDTA	--	--	--	-	---
Tris-EDTA	--	--	-	-	---
Distilled Water	--	--	-	-	---

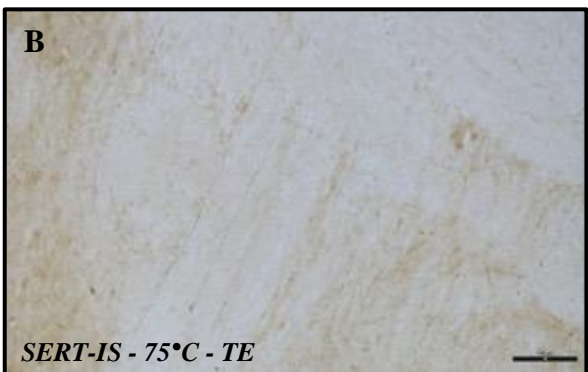
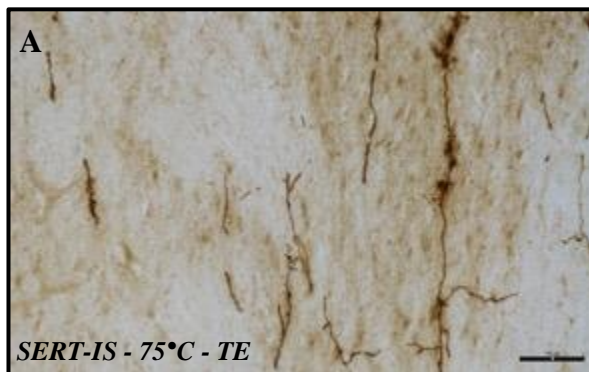
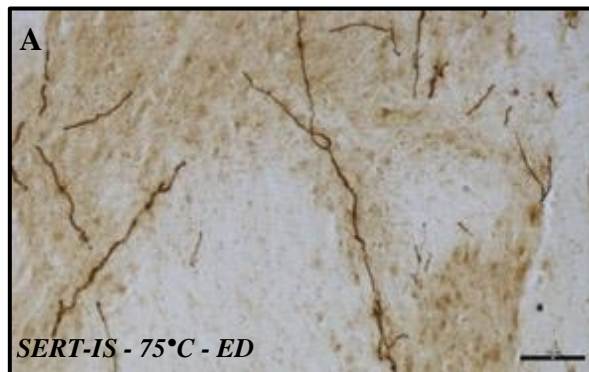
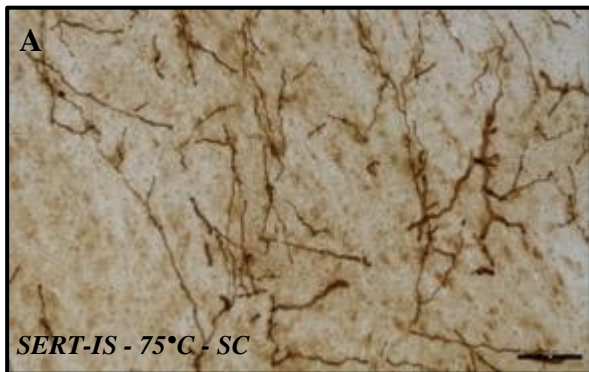
Table 8: Determination of the most optimal immersion buffer and their performance at various temperatures with regards to background staining/noise for SERT-IS (1:5000). 0.1M Sodium citrate buffer at neutral pH (pH 6.0) – SC, 0.01M EDTA buffer at high pH (pH 8.0) – ED & low molarity and 0.1M Tris-EDTA buffer at the most basic pH (pH 9.0) – TE were used as test carrier immersion buffers. Distilled water used as the control to test for the effect of temperature on the tissue slices. The background staining is rated on a scale of (-, --, ---) representing, high background noise, medium background noise, and low background noise respectively.

PT	MnR
----	-----



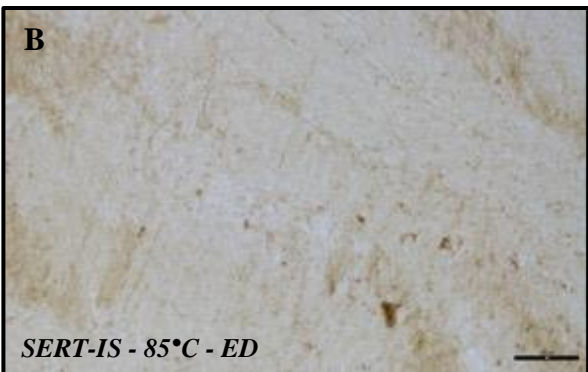
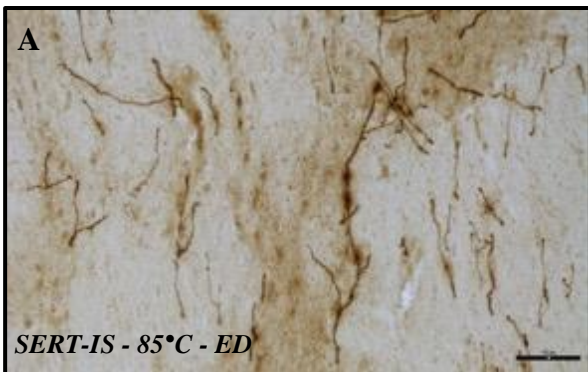
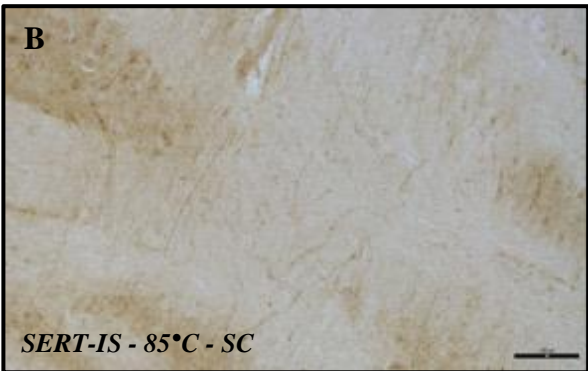
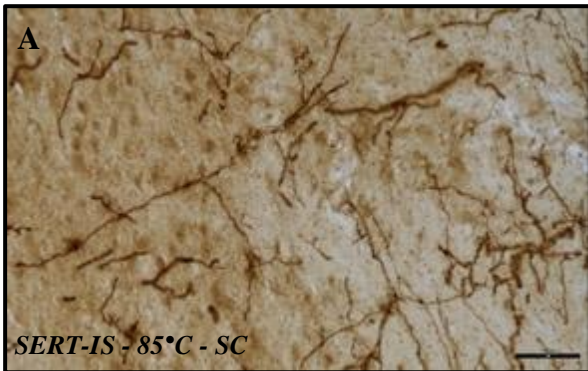


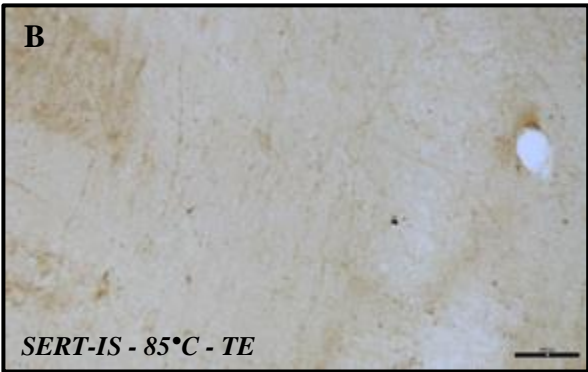
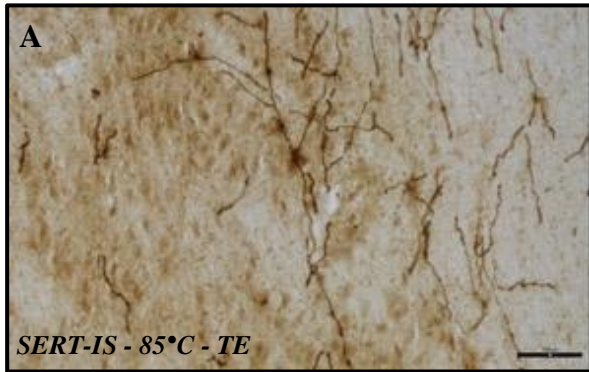
PT MnR



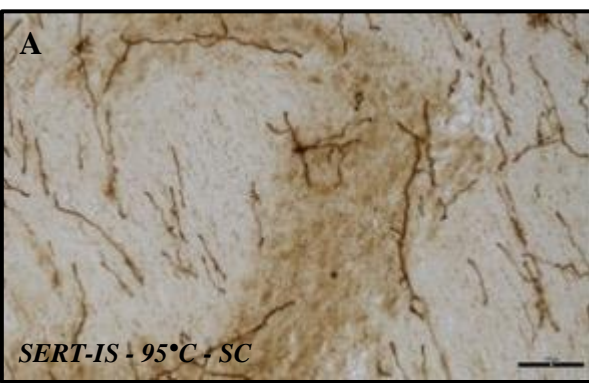


PT	MnR
----	-----





PT MnR



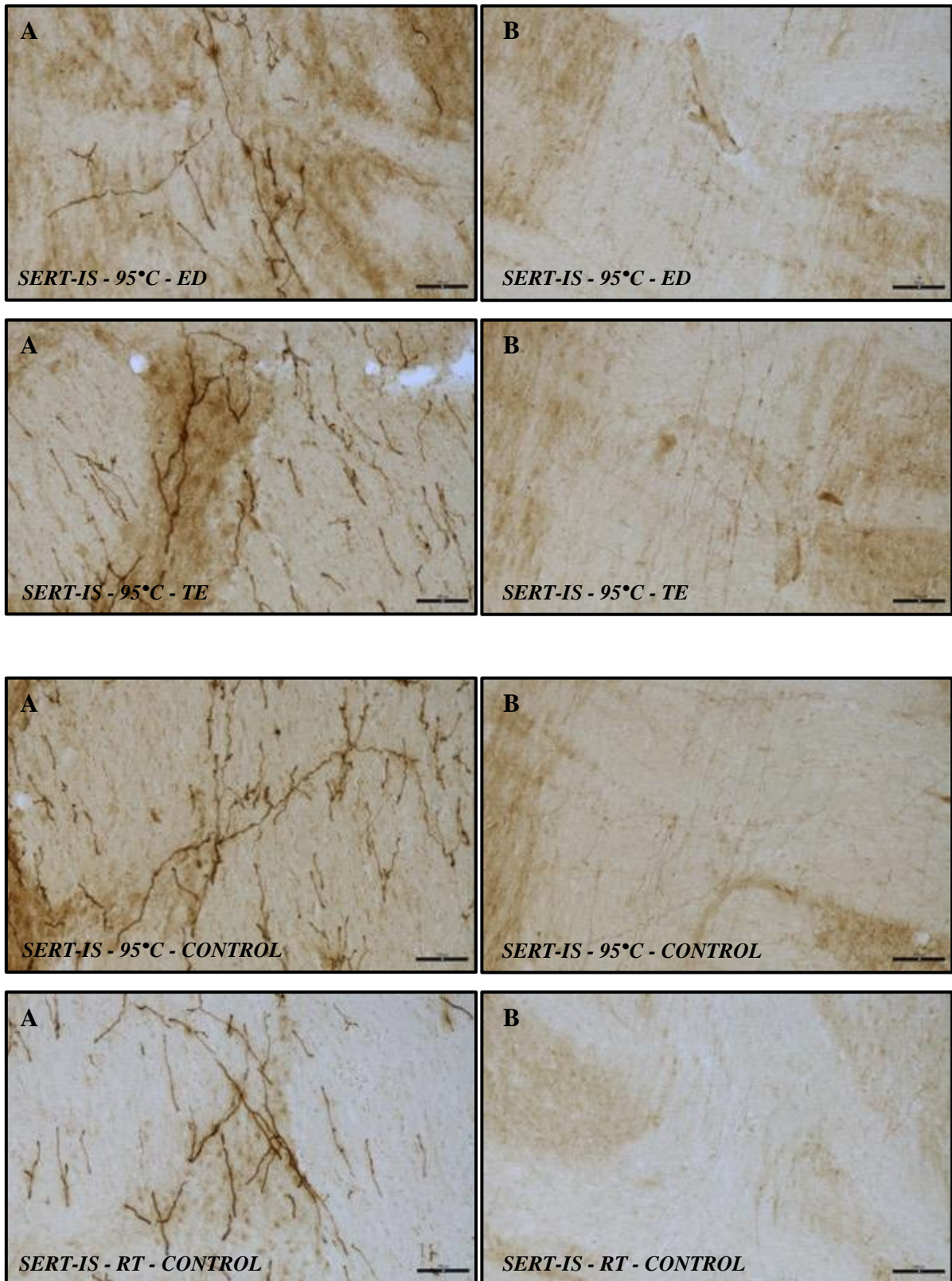


Figure 10: *Antigen retrieval buffers and their performance at various temperatures with regards to fiber definition and visualisation of the fiber bundles for SERT-IS (1:5000). 0.1M Sodium citrate buffer at neutral pH (pH 6.0) – SC, 0.01M EDTA buffer at high pH (pH 8.0) – ED & low molarity and 0.1M Tris-EDTA buffer at the most basic pH (pH 9.0) – TE were used*

as test carrier immersion buffers. Distilled water used as the control to test for the effect of temperature on the tissue slices. Columns A and B correspond to the pyramidal tract (PT) and the median raphe (MnR) respectively as per the Olszweski and Baxter's Human Brainstem Atlas.

Buffer	65°C	75°C	85°C	95°C	RT
Sodium Citrate	-	+	+	+	0
EDTA	-	+	+++	++	0
Tris-EDTA	-	+	++	+	0
Distilled Water	-	+	+	+	0

Table 9: Determination of the most optimal immersion buffer and their performance at various temperatures with regards to fiber definition and visualisation of the fiber bundles for SERT-IS (1:5000). 0.1M Sodium citrate buffer at neutral pH (pH 6.0) – SC, 0.01M EDTA buffer at high pH (pH 8.0) – ED & low molarity and 0.1M Tris-EDTA buffer at the most basic pH (pH 9.0) – TE were used as test carrier immersion buffers. Distilled water used as the control to test for the effect of temperature on the tissue slices. Fiber definition is defined as how clearly the fiber bundles and their pathways are visible from the background at 10x magnification. Visibility of both the fiber types and the clarity of their projection patterns are rated on a scale of (0, -, +, ++, +++) representing, neutral/control (low definition-with low background staining), low definition-with high background staining, high definition-with high background staining, high definition-with medium background staining and high definition-with low background staining respectively.

Buffer	65°C	75°C	85°C	95°C	RT
Sodium Citrate (Wrinkles)	-	+	+	++	-
EDTA (Wrinkles)	-	++	++	++	-
Tris-EDTA (Wrinkles)	+	++	++	+++	-
Distilled Water (Wrinkles)	-	+	+	++	-
Sodium Citrate (Tears)	-	-	-	-	-

<i>EDTA (Tears)</i>	-	-	-	-	-
<i>Tris-EDTA (Tears)</i>	-	-	+	+	-
<i>Distilled Water (Tears)</i>	-	-	-	+	-

Table 10: Determination of the effect of buffer & pH and temperature in introducing folds and wrinkles as artefacts and in increasing the fragility of the sections leading to the possibility of microtears for SERT-IS (1:5000). 0.1M Sodium citrate buffer at neutral pH (pH 6.0) – SC, 0.01M EDTA buffer at high pH (pH 8.0) – ED & low molarity and 0.1M Tris-EDTA buffer at the most basic pH (pH 9.0) – TE were used as test carrier immersion buffers. Distilled water used as the control to test for the effect of temperature on the tissue slices. Wrinkles are defined as the folding up of the tissue slice caused due to one of the factors causing tissue shrinkage and tears are when as an outcome of the fragility introduced by the specific antigen retrieval treatments. Wrinkles are rated on a scale of (-, +, ++, +++) representing absent, low (1 wrinkle), medium (2-4 wrinkles) or high (5+ wrinkles) respectively. Tears are rated on a scale of (-, +, ++, +++) representing absent, low (1 microtear at the edge), medium (2-4 microtears at the edges) or high (complete clear tear within the section) respectively.

The 0.01M EDTA (pH 8.0) buffer applied at 85°C for a duration of 20 minutes to 50µm thick slices generated the most optimal and consistent results with the anti-SERT (IS) antibody. High pH with a low molarity buffer composition positively impacted fiber and cellular staining by increasing the staining intensity at a lower temperature and by keeping the background staining usually seen with this temperature quite low. Fiber definition of both M- and D-type fibers were clearly visible at 10x magnification when subjected to this protocol. Subjecting the tissue slices to 95°C gave poorer fiber definition and increased the chances of tissue folding and wrinkling as well.

4.3 Standardise and develop an optimal protocol for the visualisation of serotonergic cell bodies and fibre tracts by modifying standard immunohistochemical protocols.

The standard immunohistochemical protocol routinely followed for unperfused tissue slices involve five major steps – quenching, blocking, primary antibody (conjugated or unconjugated to biotin), secondary antibody (if primary was unconjugated), Avidin-Biotin Complex (ABC) intensification step and finally the revealing step. The most routinely used technique for

revealing the staining is by peroxidase oxidation method using DAB or TMB as the chromogens.

Compiling the different IHC techniques used, the basic IHC framework established in our laboratory is as follows –

PARAMETERS	VARIANTS		Incubation Times		Solution Used
Quenching	1.5% H ₂ O ₂		20 mins @ RT		0.1M PBS
Blocking	0.3% Triton	5% BSA	1 hr @ RT		0.1M PBS
Primary Antibody	0.1% Triton	2% BSA	Overnight (18 hours @ 4°C)		0.1M PBS
Secondary Antibody	0.1% Triton	2% BSA	1 hr @ RT		0.1M PBS
ABC	0.1% Triton	2% BSA	1 hr @ RT		0.1M PBS
Revealing Step	DAB	Ni-DAB	15 mins	9 mins	0.05M TBS

Using this protocol as the base, systematic modifications were made within this framework to optimise the immunohistochemical protocol for each chemical marker described below. Standardisation of each parameter ensured that the best, consistent, quality, and efficient staining is achieved each time with human brainstem tissue for these specific markers, when stored and processed as described previously. The following table represents in brief, the overall titration scheme.

PARAMETERS	VARIANTS (BLOCKING STEP)						
Treatment Solution	0.1M PBS	0.05 M TBS					
Triton Concentration	0.0025%	0.005%	0.05%	0.1%	0.2%	0.3%	0.5%

BSA Concentration	5%	10%					
Anti-Secondary Serum Concentration	3%	5%	10%				
Incubation Times	1 hr @ RT	1 hr 30 mins @ RT	2 hrs @ RT				

PARAMETERS	VARIANTS (PRIMARY ANTIBODY)						
Treatment Solution	0.1M PBS	0.05 M TBS					
Triton Concentration	0.0025%	0.005%	0.05%	0.1%	0.2%	0.3%	0.5%
BSA Concentration	2%	3%	5%	10%			
Anti-Secondary Serum Concentration	2%	3%	5%	10%			
Incubation Times	Overnight (18 hours @ 4°C)	24 hrs @ 4°C	48 hrs @ 4°C	72 hrs @ 4°C	1 hr @ RT + 22 hrs @ 4°C + 1 hr @ RT	1 hr @ RT + 46 hrs @ 4°C + 1 hr @ RT	2 hrs @ RT + 44 hrs @ 4°C + 2 hrs @ RT

Primary Antibody Concentration	Start for the vendor's recommended concentration and vary based on the results. Usually 1:1000 was taken as a good starting point. Final concentration – anti-TPH2 (1:5000) and anti-SERT (IS) (1:5000). SERT (Millipore-MP) (1:5000) was also standardised but was later discarded due to comparatively inferior staining and increased artefacts.
---------------------------------------	--

PARAMETERS	VARIANTS (SECONDARY ANTIBODY)						
Treatment Solution	Use the solution that the primary antibody was made in.						
Triton Concentration	0.0025%	0.005%	0.05%	0.1%	0.2%	0.3%	
BSA Concentration	2%	3%	5%	10%			
Anti-Secondary Serum Concentration	2%	3%	5%	10%			
Incubation Times	1 hr @ RT	1 hr 30 mins @ RT	2 hrs @ RT				
Secondary Antibody Concentration	The standard established laboratory concentration of 1:250 was used for all antibodies.						

PARAMETERS	VARIANTS (ABC)						
Treatment Solution	Use the solution that the primary antibody was made in.						
Triton Concentration	0.0025%	0.005%	0.05%	0.1%	0.2%	0.3%	
BSA Concentration	2%	3%	5%				

Anti-Secondary Serum Concentration	2%	3%	5%				
Incubation Times	1 hr @ RT	1 hr 30 mins @ RT	2 hrs @ RT				
ABC Concentration	The standard established laboratory concentration of 1:100 of Reagent A and Reagent B of the ABC Universal Kit was used for all antibodies.						

PARAMETERS	VARIANTS
Treatment Solution	Use the solution that the primary antibody was made in.
Incubation Times (DAB)	Sections are tested for a range starting from 10 to 15 mins and the most optimal time is recorded to be used for successive staining. Timings may vary across antibodies for similar tissue size and architecture.
Incubation Times (Ni-DAB)	Sections are tested for a range starting from 5 to 9 mins and the most optimal time is recorded to be used for successive staining. Timings may vary across antibodies for similar tissue size and architecture.

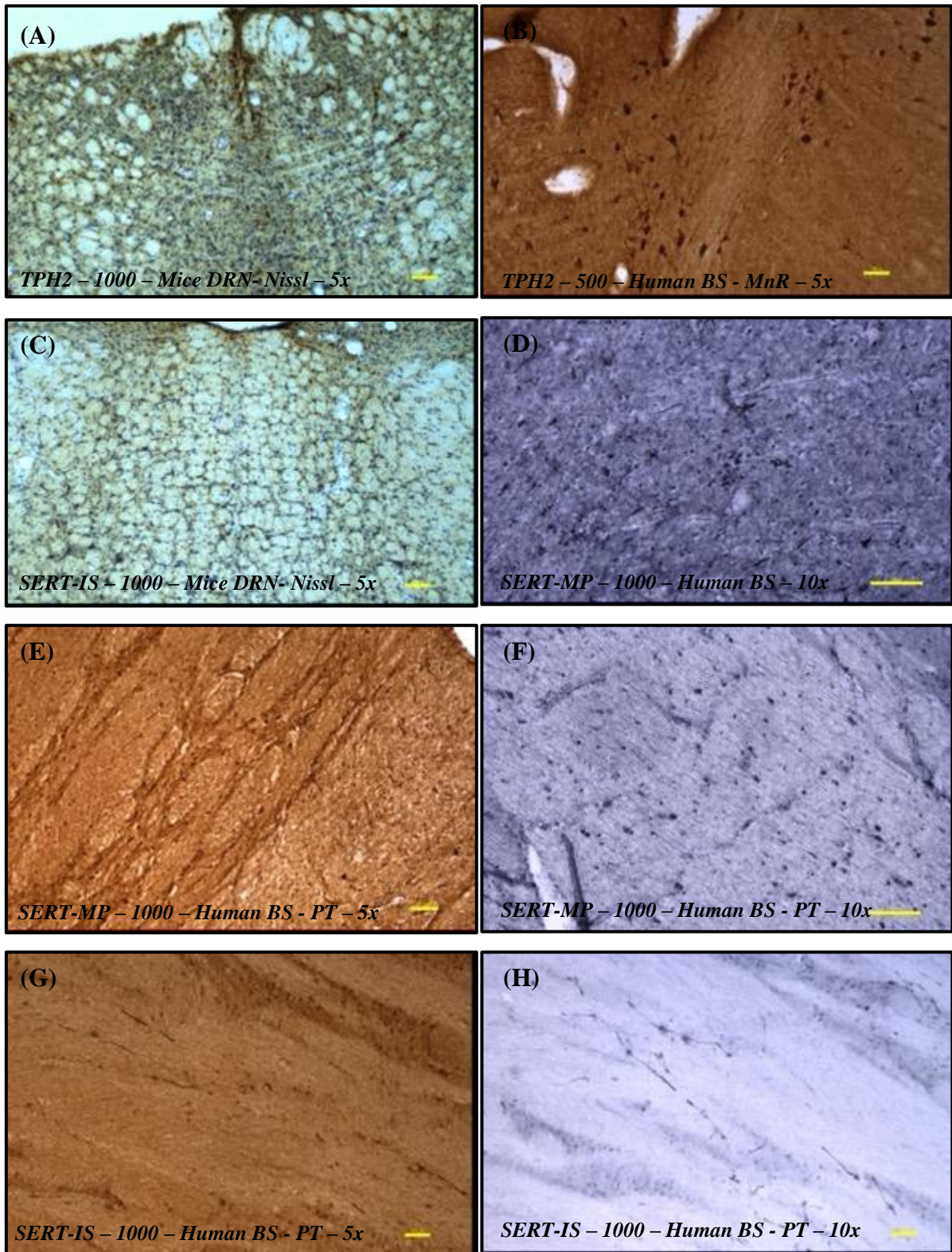


Figure 11: *Representative suboptimal staining images acquired using the previously established standard laboratory protocol for the serotonergic system. (A) Very poor staining of the serotonergic cells can be observed in perfused mice DRN even when higher antibody concentrations (Tryptophan hydroxylase – 2) of 1:1000 were used. These sections represented here are also counterstained for Nissl bodies. (B) A protocol with higher triton concentration*

(0.5%) and longer incubation time (72 hours) gave suboptimal but better staining of the serotonin cell bodies using the same antibody (TPH2) at high concentration (1:500) in human tissue at the level of the DRN. High levels of background staining can be observed with this protocol. Cellular definition and proximal dendrites are not clearly visible. (C) Extremely poor staining of the serotonergic fibers and cell bodies can be observed in perfused mice DRN even when higher antibody concentrations (Serotonin Transporter - ImmunoStar) of 1:1000 were used. These sections represented here are also counterstained for Nissl bodies. Using different SERT antibodies (MP – Millipore Sigma and IS – ImmunoStar) and revealing the fiber staining with DAB and the more sensitive Ni-DAB protocols, extremely poor staining can be seen across both antibodies (D-H). High levels of background are present in all sections with the SERT-IS giving a relatively better profile of fibers in (G, H) but nonetheless gravely underrepresenting the innervation profile of the serotonergic system. The region PT corresponds to the pyramidal tract as per the Olszewski and Baxter's Human Brainstem Atlas.

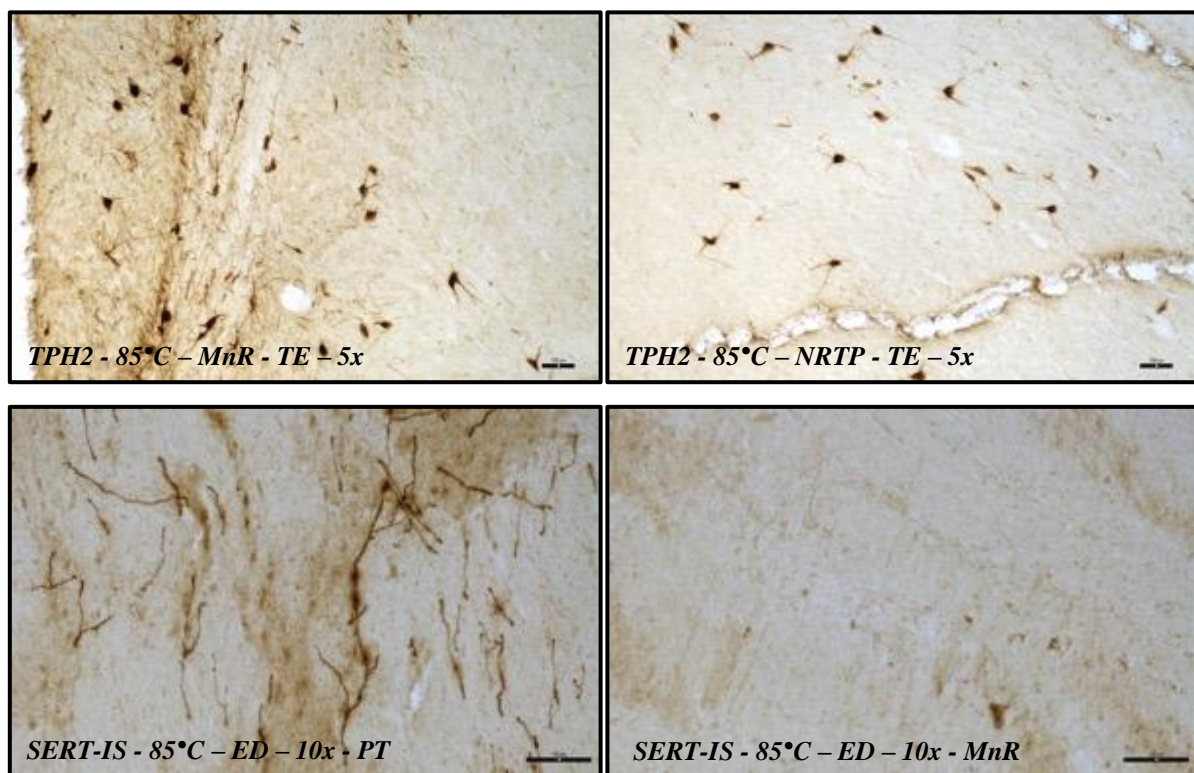


Figure 12: Representative optimal staining images – cellular and fiber bundle visualisation achieved by systematically determining and optimising the factors for the individual antibodies – TPH2 (1:5000) and SERT-IS (1:5000) for the visualisation of serotonergic system while reducing background noise and non-specific staining. Regions corresponding to the median raphe (MnR), the nucleus reticularis tegmenti pontis (NRTP), pyramidal tract

(PT) and the ventral laminae of the principal olive (VL) according to the Olszewski and Baxter's Human Brainstem Atlas are represented here.

Optimal immunohistochemical staining protocols for the target epitopes were developed, by sequentially varying all possible parameters – detergent concentration, primary & secondary serum concentrations, incubation times & temperatures. Two specific protocols for both anti-TPH2 and anti-SERT (IS) antibodies were developed. The final optimal parameters for the two antibodies are as follows –

For anti-TPH2 -

PARAMETERS	VARIANTS		Incubation Times	Solution Used
Quenching	1.5% H ₂ O ₂		20 mins @ RT	0.1M PBS
Blocking	0.3% Triton	5% BSA	2 hrs @ RT	0.1M PBS
Primary Antibody	0.2% Triton	3% BSA + 3% NHS	2 hrs @ RT + 44 hrs @ 4°C + 2 hrs @ RT	0.1M PBS
Secondary Antibody	0.2% Triton	3% BSA + 3% NHS	2 hrs @ RT	0.1M PBS
ABC	0.2% Triton	3% BSA + 3% NHS	2 hrs @ RT	0.1M PBS
Revealing Step	DAB		15 mins	0.05M TBS

For anti-SERT (IS) -

PARAMETERS	VARIANTS		Incubation Times	Solution Used
Quenching	1.5% H ₂ O ₂		20 mins @ RT	0.1M PBS
Blocking	0.3% Triton	5% BSA	2 hrs @ RT	0.1M PBS
Primary Antibody	0.2% Triton	3% BSA + 3% NGS	2 hrs @ RT + 44 hrs @ 4°C + 2 hrs @ RT	0.1M PBS

Secondary Antibody	0.2% Triton	2% BSA + 2% NGS	2 hrs @ RT	0.1M PBS
ABC	0.2% Triton	2% BSA + 2% NGS	2 hrs @ RT	0.1M PBS
Revealing Step	DAB		15 mins	0.05M TBS

CHAPTER 5: DISCUSSION AND CONCLUSION

5.1 Discussion

To gain insight into the functions of a neurotransmitter system, understanding its neuroanatomical organisation based on chemical profiles have proven to be critical [Frazer A. et al., 1999]. But visualising the serotonergic system in human post-mortem tissue using immunohistochemical methods has been challenging for over the past 4 decades. Suboptimal methodologies used in practice has led to significant contradictions in the estimates of serotonergic cells in normal human specimen and its cellular losses in neurodegenerative diseases such as PD and in healthy ageing. Developing an optimal, systematically standardised immunohistochemical protocol for visualising the serotonergic neurons in human tissue would potentially address these contradictions and methodological deficiencies. With the significant challenges that are associated with the application of immunohistochemistry to the human serotonergic system, pre-immunohistochemical measures must be adopted, standardised, and optimally applied to achieve quality, reproducible immunohistochemical staining. Here, I have proposed and determined whether antigen retrieval techniques increase the sensitivity and morphological visualisation of the serotonergic neurons and their fiber projections with the anti-TPH2 and anti-SERT (IS) antibodies as cellular and fiber markers respectively.

A human serotonergic dataset created based on immunohistochemical staining must provide uniform staining across the entire tissue, with staining intensities only actively reflecting the inherent regional tissue variations instead of giving out false negatives and positives. Here, antigen retrieval proves critical for the quality control and standardisation of the immunohistochemical staining [Tacha D. & Teixeira M., 2013]. The type of fixative used to preserve the tissue, temperature and the duration of fixation are factors that significantly influence immunostaining. Since the effect of these storage solutions on the various epitopes are not uniform and varies significantly, adequate unmasking of the target epitope with specific retrieval methods must be applied to achieve optimal immunohistochemical staining for the visualisation of that specific target epitope. Implementation of optimal antigen retrieval measures provide clear visualisation of regional fiber type innervation patterns and an increased sensitivity of cellular profiles. This may allow for improved and more accurate quantification. With increased antibody sensitivity, a significant reduction in antibody costs is also observed which would prove to be significant when applied to the creation of histological datasets.

HIER is a pre-immunohistochemical procedure for enhancing immunohistochemical detection [Sharma et al., 1990; Shin et al., 1991; Shi et al., 1991]. Properties of temperature, pH, buffer, molarity, and the method of application of HIER significantly affect the efficacy of HIER. Due to the lack of a universal retrieval buffer that can be optimally applicable to all tissue epitopes, a standard HIER protocol applicable to all tissue and epitope types is not available. Hence, it becomes crucial to identify and choose the method that works specifically for the antibody of interest.

Factors affecting epitope unmasking

1. Formalin fixation

Although formalin is an excellent fixative for immunohistochemistry, extended fixation using formalin damages antigens in addition to inducing secondary molecular cross-links in proteins i.e., methylene bridges [D'Amico, F., Skarmoutsou, E., & Stivala, F., 2009]. This change in the three-dimensional structure of the epitope makes it difficult for the antibody to bind to its target. The total duration of fixation directly affects the amount of antigen damage, with longer durations causing more damage and increased secondary cross-links. Formalin fixation tends to generate many hydroxymethyl groups that link to protein groups. This allows for the formation of strong bonds between proteins and calcium ions forming a “cage-like complex”. Application of an appropriate antigen retrieval method overcomes this problem.

2. Antigen Retrieval techniques – Heat Induced Epitope Retrieval (HIER) and Enzyme Induced Epitope Retrieval (EIER - Protease Digestion)

Enzyme Induced Epitope Retrieval (EIER) employs the application of proteolytic enzymes such as trypsin, ficin, proteinase K, pepsin, pronase, DNase etc. The epitope is allowed to assume its native conformation after the proteolytic cleavage of the molecular links that were induced during tissue fixation. Even though EIER is an effective method for antigen unmasking, it is a harsh treatment and often negatively affects the target epitope and significantly affecting the background staining. Increased “muddy” staining can be seen with several antibodies. Application of this method must be considered a last resort when the gentler method of heat induced epitope retrieval does not work.

Heat Induced Epitope Retrieval (HIER) is the antigen retrieval method most commonly applied in immunohistochemistry. The target tissue is subjected to heat via solutions of various compositions to return the epitope back to its three-dimensional conformation and break the

molecular cross-links induced by formalin. Although currently the mechanism of action of HIER is not fully understood, some studies suggest that precipitation of tissue bound calcium and other divalent cations may play some role in it [Morgan J.M. et al., 1994; Yaziji H. et al., 1997]. As formalin fixation is thought to allow for the formation of strong bonds between proteins and calcium ions forming a “cage-like complex”, calcium-chelating agents may act as effective epitope retrieval buffers. Another method of action of HIER might be via the restoration of bound water to protein structures, returning the epitope to a more native state. This hypothesis was developed after observing the benefit of applying HIER to tissues subjected to alcohol fixation [Gown A.M. et al., 1993; Suurmeijer A.J.H. & Boon M.E., 1993]. Alcohol fixation does not induce extensive cross-linking of proteins, but since it is a dehydrating fixative, it induces its effect by removing the water molecules that are non-covalently bound to the amino acid side chains. Removal of these bound water molecules is thought to potentially affect the native three-dimensional conformation of the protein.

Hence many different buffers have been employed for the retrieval of masked epitopes. 0.1M sodium citrate buffer (pH 6.0), 0.01M EDTA (pH 8.0), 0.1M Tris-EDTA (pH 9.0), incubation buffers (PBS; TBS) and distilled water have been routinely applied for antigen retrieval. Many other factors affect the success of epitope retrieval i.e., temperature, duration of application, heat source, carrier solution used - buffer (pH and ionic strength) or distilled water. Due to the lack of a universal retrieval buffer, and the varying ways in which the fixative might have affected the target epitope, retrieval methodologies must be evaluated and standardised for each epitope of interest.

Comparing the efficacy of HIER protocol on tissue blocks and free-floating sections

To determine the most effective stage of HIER application, a comparative study identifying the efficacy of HIER across tissue blocks – Large (3x2x5 cm³ approx.) and small (3x2x2 cm³ approx.) and 50µm thick tissue slices was performed. Using anti-TPH2 and anti-SERT as markers for serotonin immunohistochemical sensitivity, tissue regions from the same brain sample and across different brain samples were compared. A more intense and uniform staining was observed on 50µm tissue slices that had undergone the antigen retrieval procedure post generation of the slices when compared to the application of the antigen retrieval procedure to tissue blocks prior to tissue slicing. Between the large and small tissue blocks, the slices generated from the smaller block showed more uniform staining patterns when compared to

the larger blocks. More background staining was also observed in the tissue slices generated from the larger blocks. Tissue thickness also seemed to slightly affect the introduction of wrinkles during mounting. Although the antigen retrieved 50µm thick tissue slices did not prove any more difficult to mount when compared to the antigen retrieved slices from the small and large tissue blocks, they did carry a tendency to fold over and caused few wrinkles. The tissue slices generated from tissue blocks of HIER did not show any form of structural/tissue integrity compromise or introduction of folds. Overall, performing the antigen retrieval on 50µm thick tissue slices was the most optimal as uniform and sufficient penetration of the retrieval buffer into the slices was achieved, leading to uniform unmasking of the target epitopes. The small and large blocks allowed for insufficient penetration of the antigen retrieval buffer causing variable unmasking. The tissue temperature for the internal regions potentially might not have reached the target 90°C when incubated for a duration 20 mins while keeping the solution longer at such high temperatures may damage the external tissue surface. A combination of poor antigen retrieval buffer penetration and an inadequately raised internal temperature might contribute to the poor and inconsistent staining of serotonin cells with anti-TPH2 with the presence of higher background noise.

Effect of temperature on HIER on staining intensity, definition, and tissue structural integrity

To identify the relationship between temperature and epitope unmasking efficacy and the most effective temperature on tissue slices, a range of temperatures - 60°C to 100°C were tested. A direct relationship between temperature and serotonin cellular staining could be seen. With increasing temperatures, increased staining intensity and cellular definition was achieved. But this also came at the cost of a significant increase in background staining with the increasing temperatures. The highest staining intensity was achieved with the application of heat at the temperature of 95°C, but with very high background staining as well. Staining at 85°C provided similar cellular staining definition but with lower cellular and fiber staining intensity. But this temperature also produced less background staining as compared to the tissue slice subjected to 95°C heat. This lower temperature also reduces the potential introduction of fold & wrinkles and the possibility of compromising tissue integrity. When comparing the range of effective temperatures for antigen retrieval and how they affect the structural integrity of the tissues, it was observed that the structural integrity of the tissue is challenged at the temperature of 95°C. Wrinkles and folds are introduced at this temperature, with the tissue carrying a tendency to

shrink. Even though this unwanted secondary effect did not bear much impact on its successful subsequent IHC staining and mounting, the folds and the wrinkles would introduce unwanted artefacts if those tissue slices were to be used for a 3D histological reconstruction for the purpose of creating an atlas. Hence, using the lower temperature of 85°C seems to provide the benefits of improved staining without introducing any significant wrinkles, folds or compromising the tissue slice structural integrity.

Effect of high- and low-pH antigen retrieval buffers on IHC staining with varying temperatures

To determine the effect of different antigen retrieval buffers and varying pH (low and high) on its epitope unmasking capabilities, 0.1M Sodium Citrate (pH 6.0), 0.01M EDTA (pH 8.0) and 0.1M Tris-EDTA (pH 9.0) buffers were tested. For the anti-TPH2 marker, the 0.1M Tris-EDTA (pH 9.0) buffer applied at 85°C for a duration of 20 minutes to 50µm thick slices generated the most optimal and consistent results. Increased pH in combination with the buffer composition positively impacted cellular staining by reducing the increased background staining that was observed with the increase in the temperature. Even though subjecting the tissue slice to 95°C gave more intense staining, it also came with the drawbacks of tissue folding and wrinkling. For the anti-SERT (IS) marker, the 0.01M EDTA (pH 8.0) buffer applied at 85°C for a duration of 20 minutes to 50µm thick slices generated the most optimal and consistent results. High pH with a low molarity buffer composition positively impacted fiber and cellular staining by increasing the staining intensity at a lower temperature and by keeping the background staining usually seen with this temperature, low. Fiber definition of both M- and D-type fibers were clearly visible at 10x magnification when subjected to this protocol. Subjecting the tissue slice to 95°C gave poorer fiber definition and increased the chances of tissue folding and wrinkling as well. Simultaneously, optimal immunohistochemical staining protocols for the target epitopes were developed, by sequentially varying all possible parameters – detergent concentration, primary & secondary serum concentrations, incubation times & temperatures. Two specific protocols for both anti-TPH2 and anti-SERT (IS) antibodies were developed.

5.2 Limitations

Effect of 4%PFA fixation duration

Due to the lack of availability of human post-mortem tissue for testing, the tests were all carried out mainly from one brainstem. Testing on tissues stored for varying incubation durations in 4% PFA would identify its effect on epitope masking and how it varies with respect to time and its regional variability, improving the strength of the study.

Stereological analysis and low sample size

Having a higher sample size, from different brains, the study would have benefitted from being able to control for any age-related differences inherent to the tissue specimen. Performing stereological analysis and quantifying the cell counts in addition to the qualitative analysis performed here, would have increased the strength of the study, and provided a quantitative measure for the regional variabilities observed.

Effect of HIER on endogenous biotin

One of the challenges of applying HIER is the possibility of increased background staining due to the enhanced reactivity of endogenous biotin. Using an avidin-biotin detection system might lead to increased artefacts. Endogenous biotin is present in all metabolically active cells. Intensification of this free biotin with the application HIER appears as a “muddy” cytoplasmic reactivity without any clear visible cellular profiles outlined. Depending on the HIER solution used, endogenous biotin shows variable enhancement. Tris buffered solutions tend to generate stronger artefacts when compared to citrate buffers. But this effect must be identified and standardised to each epitope and target tissue by varying the HIER solution.

5.3 Conclusion

The above experiments demonstrate that antigen retrieval is critical for the successful immunohistochemical localisation of target epitopes if tissues are preserved for long durations in formalin or paraformaldehyde. Since formalin cross-linking masks tissue antigens, antibody access and recognition of active sites is hampered. Such cross-links can be reversed by placing the fixed tissues in different types of retrieval buffers and heating it. Heat-induced antigen retrieval (HIER) and enzymatic antigen retrieval techniques are the most common methods of reversing such cross-links. Between the two methods, the enzymatic retrieval provides improved staining at the cost of tissue digestion, deteriorating tissue quality and morphology, limiting its use. Comparative studies of different HIER techniques using other protocols have

also shown that heat is the key factor in delivering successful antigen retrieval [**Tacha D. & Teixeira M., 2013**]. There is a crucial, time-temperature association where longer exposure to higher temperatures increases the unmasking of the antigens, thus giving better immunohistochemical staining. But high temperatures also negatively impact the morphology and the quality of the processed tissue, subsequently affecting tissue staining and preservation. Among the different heat-induced antigen retrieval techniques available, the boiling water bath technique preserves tissue morphology, is gentle on the tissue and gives a uniform, constant HIER treatment [**Tacha D. & Teixeira M., 2013**]. Different tissue types based on their fixation duration require differing antigen retrieval treatments, especially for low-expression or high-sensitivity markers. Hence, standardising the protocols for individual tissue types with considerations to pH, time and type of buffer used, specific to the target epitope and its antibody is a critical step in the development of histological datasets.

5.4 Perspective - Serotonin, Atlases and Parkinson's Disease

Serotonin system – A role in Parkinson's Disease

Parkinson's Disease (PD) is known as a debilitating progressive neurodegenerative disorder, which has been characterized by a loss of nigrostriatal dopaminergic neurons in the SN_c [**Nayyar T. et al., 2009; Braak H., Del Tredici K. et al., 2003; Braak, H., Ghebremedhin E. et al., 2004**]. Although nigrostriatal dopaminergic degeneration is implicated in the motor symptoms - bradykinesia, rigidity and tremor, the pathophysiology of non-motor symptoms of PD - depression, impulsivity, anxiety, and sleep disturbances are far less known. These non-motor symptoms are attributed to the impaired functioning of non-dopaminergic cells, especially to those of the pontine serotonergic (5-HT) system although only the Lewy pathology (LP) in the dopaminergic SN_c garners much of the attention [**Bosboom J.L.W. et al., 2003; Halliday G.M., Leverenz J.B. et al., 2014; Huot P. & Fox S.H., 2013; Riekkinen M., Kejonen K. et al., 1998; Sawamoto N., Piccini P. et al., 2008; Buddhala C. et al., 2015**]. Heiko Braak and colleagues proposed the hypothesis of an ascending early brainstem disease to cortical pathology, of an advancing PD, based on the appearance of LP at various stages from Hoehn-Yahr (I-V) [**Braak H., Del Tredici K. et al., 2003; Braak, H., Ghebremedhin E. et al., 2004**]. This converging data of the role of brainstem nuclei in the early prodromal non-motor symptoms, the staging of Braak's hypothesis and the theory of global bioenergetic failure characterizing these specific neuronal losses, suggests a critical role for the brainstem nuclei in the progression of the PD pathology. Nonetheless, contradicting evidence of the absence of systematic LP in PD, presence of LP in healthy ageing individuals and the loss of

SNC neurons in the absence of LP in the case of early-onset genetic PD has been observed. Although there is a consensus regarding the loss of serotonergic nuclei in PD based on the deposition of LBs as observed by Heiko Braak and others [Ohama E. & Ikuta F., 1976; Mann D.M. & Yates P.O., 1983; Halliday et al., 1990a; Halliday et al., 1990b; Paulus W. & Jellinger K., 1991], limited studies have used chemical markers to specifically quantify the pattern of degeneration of specific brainstem serotonergic cell groups, their projections in PD and their relationship to LP pathology. At present, there are also significant contradictions in the estimates of serotonergic cell loss in PD with one stereological study suggesting no cell loss in the dorsal raphe nucleus (DRN) while others have observed between 50-90% serotonin cell loss in the DRN and the median raphe nucleus (MRN) [Giguère, N. et al., 2018].

Neuronal loss in the dorsal raphe nucleus was found to be more significantly affected in depressed PD patients when compared to non-depressed PD patients [Huot P. & Fox S.H., 2013]. But no such preference for specific serotonergic nuclei were shown in any of the other PD types – demented vs non-demented, psychotic vs non-psychotic and akinetic-rigid vs tremulous PD patients [Huot P. & Fox S.H., 2013; Paulus W. & Jellinger K., 1991; Frisina P.G. et al., 2009]. Comparative studies have shown that the caudate is more serotonergically denervated than the putamen whereas the inverse phenomenon is observed with the dopaminergic system [Fahn S., 2008; Kish S.J. et al., 2008; Wilson J.M. et al., 1996]. The patterns of serotonergic cell loss have been suggested to play a significant role in the development of dyskinesias. The emergence of L-DOPA induced dyskinesias (LIDs) is believed to be the consequence of 5-HT terminals in striatum acting as false neurotransmitters of dopamine (DA) by taking up L-DOPA, metabolising it to DA via the enzyme L-aromatic amino acid decarboxylase (AADC) culminating in its unregulated release [Cheshire P. et al., 2015]. The role of serotonergic nuclei in the successful maintenance of the dyskinesic state was further investigated in dual lesioning studies of the nigrostriatal dopaminergic and rostral raphe-striatal serotonergic inputs [Eskow K. L., et al., 2009]. These studies indicated the prominent role played by the serotonergic system leading to the development of LIDs. Contrastingly, **Buddhala C. et al (2015)** noted that, regional reductions in 5-HT correlated with that of SERT, which contrasts with the LIDs origin hypothesis.

Among the non-motor symptoms, cognition and psychiatric changes observed in PD are possibly linked to alterations in multiple neurotransmitter systems [Bosboom J.L.W. et al., 2003; Halliday G.M., Leverenz J.B. et al., 2014; Huot P. & Fox S.H., 2013; Riekkinen M.,

Kejonen K. et al., 1998; Sawamoto N., Piccini P. et al., 2008]. In advanced PD with dementia, widespread deficits in the dopaminergic, serotonergic, and noradrenergic systems were observed using HPLC and ELISA techniques [**Buddhala C. et al., 2015**]. But a comparative histological analysis of the deficits among the various monoaminergic system in the basal ganglia, limbic and brainstem structures has not been performed. Investigating the extent of regional deficits in the different monoaminergic systems with regards to each other, in Parkinsonian, ageing and age matched control brains will help enable a qualitative map to be applied in future studies.

Furthermore, it is not known if serotonergic neurons degenerate prior to dopamine cell loss in early PD possibly explaining the early non-motor symptoms or if this degeneration occurs later in the disease. As per Braak's staging, the PD pathology starts affecting the raphe nuclei in stage 2 leading to the entire raphe complex being affected by stage 3 [**Braak H., Del Tredici K. et al., 2003; Braak, H., Ghebremedhin E. et al., 2004**]. Interestingly the substantia nigra and the other midbrain structures are only affected in stage 3. This earlier serotonergic neuronal susceptibility preceding dopaminergic cell loss might explain the prodromal presentation of depression and other non-motor symptoms manifested in PD. Indeed, if Braak's hypothesis is correct, we would expect early PD patients to show significant serotonergic degeneration, in keeping with the loss of trophic support from 5-HT efferents to the SN_c promoting DA degeneration. Studies have shown that lower brainstem noradrenergic afferents provide critical trophic support to DA neurons for their survival in PD [**Hassani O.K. et al., 2020**]. And since serotonin is a known trophic factor for target DA neurons, an early degeneration of 5-HT system might contribute to the observed midbrain-dopaminergic cell loss in PD, in keeping with Braak's hypothesis. Furthermore, in neurodegenerative processes, toxic increase in intracellular calcium is a major factor towards which calcium binding proteins provide a first line of defence [**Fairless R et al., 2019**]. Differential susceptibility of neurons to degenerate might indicate the importance of these calcium binding proteins as determinants of survival of specific neuronal subpopulations [**Fairless R et al., 2019; Goodman J H et al., 1993**]. Since the selective vulnerability of the various serotonergic neurons within different serotonergic nuclei in PD have not yet been documented, studying the chemical profiles of such selectively resistant/vulnerable neurons in the brainstem raphe and midbrain regions will significantly inform the scientific community about the underlying pathological progression patterns of PD. Following an improved understanding of the nuclei networks to which they connect, effective detection, targeting and management of the prodromal symptoms of PD can be achieved.

To that end, application of this optimal serotonin immunohistochemical protocol for visualising its chemo- and cyto- architectonic profiles in combination with calcium binding proteins as chemical markers, would provide us with a unique anatomical parcellation of the serotonin neuronal subpopulations, which might provide an increased understanding of the processes underlying the selective vulnerability of neurons.

Human Brain Atlases – Serotonin System

In the past couple of decades, sophisticated human brain atlas development has been urged forward by the growing cost of brain disorders and societal ageing [Nowinski W. L. 2020]. This evolution has been in part, driven by the availability of sophisticated imaging & parcellation techniques, advanced brain mapping and powerful computing. Human brain mapping has evolved over the years, from early basic hand-drawn cortical maps, print stereotactic atlases, early digital atlases to the current advanced brain atlas platforms. The earliest hand-drawn, post-mortem cortical maps by *Brodmann (1909)*, *Von Economo & Koskinas (1925)* and *Vogt and Vogt (1919)*, *Flechsig (1920)* were produced for a single modality; containing cyto- and myelo- architectonics respectively, which varied greatly in terms of the number of the parcellated cortical areas between the atlases. This was followed by the development of stereotactic atlases due to a need in neurosurgery to localise cerebral structures in the pre-tomographic imaging era.

The usefulness of a human brain atlas depends not only on the atlas content but rather on its availability and functionality, enabling and supporting various atlas-based applications. Driven by the need of the human brain mapping community in integrating structural, functional, and multi-modal images in the same stereotactic space as well as for atlas-assisted automatic labelling of activation loci in functional images with stereotactic coordinates, attempts have been made to develop atlases with increased functionality. But even in this decade of novel digital human brain atlases [Evans A. C. et al., 2012; Ding S. L. et al., 2016, Sunkin S. M., et al., 2013], system specific atlases employing ground truth measures from immunohistochemistry, spatially co-registering to other modalities in a stereotactic framework have been quite rare due to the labour-intensive nature of the work. Atlases such as the *Allen Brain Atlas* [Sunkin S. M., et al., 2013], a gene-expression atlas, provides high in-plane spatial resolution but sparse intra-plane resolution, effectively decreasing its usefulness in interpreting neuroimaging modalities due to the reduced spatial resolution. With such atlases also being

anisotropic in nature, the definitive conclusions that can be drawn becomes limited [Amunts K., Mohlberg H. et al., 2020]. These microstructural atlases although contain ground truth information, they do not possess inter-subject variability information as they usually rely on a single brain. Complementing such an atlas with other *in vivo* studies will lead to an effective understanding of the functional connectivity and its implications in pathological states.

Concurrently, the available paper atlases of human brainstem, *An atlas of the brain stem and cerebellum with surface anatomy and vascularization* by Duvernoy H.M. in 1995, *Atlas of the brainstem and cerebellar nuclei* by Afshar et al. in 1978, *Cytoarchitecture of the human brainstem* by Olszewski and Baxter in 1982, *Atlas of the human brainstem* by George Paxinos and Xu-Feng Huang in 1995 & 2019 and *Duvernoy's Atlas of the Human Brain Stem and Cerebellum (2009)* with 9.4T images of 40–60-micron resolution present the same limitations from which most second and third-generation atlases suffer [Nowinski W. L. 2020]. These include its static nature, limited functionality, sparse image frequency, lack of chemoarchitectonic features, limited parcellation criteria and the difficulty in mapping these brain-maps to individual brain scans. With the *Cytoarchitecture of the human brainstem*, Olszewski tried to portray the cytoarchitecture of all the neuronal entities in the medulla oblongata, pons, and midbrain. He successfully delineated previously undecided cell groups based on the cytoarchitectonic criterion. Nissl staining technique was used as the method of choice to visualise the cytoarchitectonic profiles. These forms of delineations presume that groups of cells delineated by such methods possess certain properties of biological significance translating into functional import as well, which may play a significant role in differential disease progression, susceptibility, and developmental characteristics. Advancing this further by integrating a chemical modality to a comprehensive cytoarchitectonic atlas [Amunts K., Mohlberg H. et al., 2020], especially at the level of the brainstem, will inform us of the selective vulnerability of neurons in specific neurodegenerative processes such as PD.

This substantiates the need to develop an ultra-high resolution, stereotactic atlas of the serotonin system, that will enable the elucidation of the patterns of serotonergic cell loss in health ageing, early PD, and late PD in the brainstem by creating quantifiable chemo-specific digitized atlases, designed for stereological chemo-specific analysis and for allowing the visualisation of its complex projections. This will identify and resolve by quantifying, if any, the correlations between the 5-HT system, LB pathology in raphe nuclei and cell loss in the midbrain dopaminergic systems. And for the development of such an atlas, the critical

components of pre-IHC and IHC must be standardised and optimised to circumvent all the challenges associated with visualising the serotonergic system immunohistochemically in the human tissue. An atlas generated as such would also serve wider uses as roadmaps to brainstem and subcortical monoaminergic systems, in research and clinical practice, if volumetrically digitized and then registered to a standard reference MRI space.

REFERENCES

- Alelú-Paz, R., Iturrieta-Zuazo, I., Byne, W., Haroutunian, V., García-Villanueva, M., Rábano, A., García-Amado, M., Prensa, L. & Giménez-Amaya, J. M. (2008). A New Antigen Retrieval Technique for Human Brain Tissue. *PLoS ONE*, 3(10), e3378. <https://doi.org/10.1371/journal.pone.0003378>
- Amunts, K., Mohlberg, H., Bludau, S. & Zilles, K. (2020). Julich-Brain: A 3D probabilistic atlas of the human brain's cytoarchitecture. *Science*, 369(6506), 988–992. <https://doi.org/10.1126/science.abb4588>
- Azmitia E. C. (1999). Serotonin neurons, neuroplasticity, and homeostasis of neural tissue. *Neuropsychopharmacology: official publication of the American College of Neuropsychopharmacology*, 21(2 Suppl), 33S–45S. [https://doi.org/10.1016/S0893-133X\(99\)00022-6](https://doi.org/10.1016/S0893-133X(99)00022-6)
- Bach H, Arango V. Neuroanatomy of Serotonergic Abnormalities in Suicide. In: Dwivedi Y, editor. *The Neurobiological Basis of Suicide*. Boca Raton (FL): CRC Press/Taylor & Francis; 2012. Chapter 2. Available from: <https://www.ncbi.nlm.nih.gov/books/NBK107204/>
- Baker, K. G., Halliday, G. M., & Törk, I. (1990). Cytoarchitecture of the human dorsal raphe nucleus. *The Journal of comparative neurology*, 301(2), 147–161. <https://doi.org/10.1002/cne.903010202>
- Berger, M., Gray, J. A., & Roth, B. L. (2009). The expanded biology of serotonin. *Annual review of medicine*, 60, 355–366. <https://doi-org.proxy3.library.mcgill.ca/10.1146/annurev.med.60.042307.110802>
- Bertrand, G., Olivier, A., & Thompson, C. J. (1974). Computer display of stereotaxic brain maps and probe tracts. *Acta Neurochirurgica Supplement*, 21, 235–243.
- Bosboom, J. L. W., Stoffers, D., & Wolters, E. C. (2003). The role of acetylcholine and dopamine in dementia and psychosis in Parkinson's disease. *Advances in research on neurodegeneration*, 185-195.

Brodmann, K. (1909). *Vergleichende Lokalisationslehre der Grosshirnrinde in ihren Prinzipien dargestellt auf Grund des Zellenbaues*. Barth.

Buddhala, C., Loftin, S. K., Kuley, B. M., Cairns, N. J., Campbell, M. C., Perlmutter, J. S. & Kotzbauer, P. T. (2015). Dopaminergic, serotonergic, and noradrenergic deficits in Parkinson disease. *Annals of Clinical and Translational Neurology*, 2(10), 949–959. <https://doi.org/10.1002/acn3.246>

Büttner-Ennever, J. A., & Horn, A. K. (Eds.). (2014). *Olszewski and Baxter's Cytoarchitecture of the human brainstem*. Basel: Karger.

Cattoretti, G., Pileri, S., Parravicini, C., Becker, M. H., Poggi, S., Bifulco, C., Key, G., D'Amato, L., Sabbatini, E., & Feudale, E. (1993). Antigen unmasking on formalin-fixed, paraffin-embedded tissue sections. *The Journal of pathology*, 171(2), 83–98. <https://doi.org/10.1002/path.1711710205>

Charnay, Y., & Léger, L. (2010). Brain serotonergic circuitries. *Dialogues in clinical neuroscience*, 12(4), 471–487. <https://doi.org/10.31887/DCNS.2010.12.4/ycharnay>

Crawford, L. K., Craige, C. P., & Beck, S. G. (2010). Increased intrinsic excitability of lateral wing serotonin neurons of the dorsal raphe: a mechanism for selective activation in stress circuits. *Journal of neurophysiology*, 103(5), 2652–2663. <https://doi.org/10.1152/jn.01132.2009>

Cuevas, E. C., Bateman, A. C., Wilkins, B. S., Johnson, P. A., Williams, J. H., Lee, A. H., Jones, D. B., & Wright, D. H. (1994). Microwave antigen retrieval in immunocytochemistry: a study of 80 antibodies. *Journal of clinical pathology*, 47(5), 448–452. <https://doi.org/10.1136/jcp.47.5.448>

Dahlström, A., & Fuxe, K. (1964). Localization of monoamines in the lower brainstem. *Experientia*, 20(7), 398-399.

D'Amico, F., Skarmoutsou, E., & Stivala, F. (2009). State of the art in antigen retrieval for immunohistochemistry. *Journal of immunological methods*, 341(1-2), 1–18. <https://doi-org.proxy3.library.mcgill.ca/10.1016/j.jim.2008.11.007>

Ding, S. L., Royall, J. J., Sunkin, S. M., Ng, L., Facer, B. A., Lesnar, P., ... & Lein, E. S. (2016). Comprehensive cellular-resolution atlas of the adult human brain. *Journal of Comparative Neurology*, 524(16), 3127-3481.

Duvernoy, H. M. (1995). *The Human Brain Stem and Cerebellum. Surface, Structure, Vascularization, and Three-Dimensional Sectional Anatomy, with MRI*. Wien: Springer.

Duvernoy's Atlas of the Human Brain Stem and Cerebellum. (2009). *AJNR: American Journal of Neuroradiology*, 30(5), e75. <https://doi.org/10.3174/ajnr.A1550>

Evans, A. C., Janke, A. L., Collins, D. L., & Baillet, S. (2012). Brain templates and atlases. *Neuroimage*, 62(2), 911-922.

Eskow, K. L., Dupre, K. B., Barnum, C. J., Dickinson, S. O., Park, J. Y., & Bishop, C. (2009). The role of the dorsal raphe nucleus in the development, expression, and treatment of L-dopa-induced dyskinesia in hemiparkinsonian rats. *Synapse (New York, N.Y.)*, 63(7), 610–620. <https://doi.org/10.1002/syn.20630>

Fahn S. (2008). The history of dopamine and levodopa in the treatment of Parkinson's disease. *Movement disorders: official journal of the Movement Disorder Society*, 23 Suppl 3, S497–S508. <https://doi.org/10.1002/mds.22028>

Fairless, R., Williams, S. K., & Diem, R. (2019). Calcium-Binding Proteins as Determinants of Central Nervous System Neuronal Vulnerability to Disease. *International journal of molecular sciences*, 20(9), 2146. <https://doi.org/10.3390/ijms20092146>

Frazer A, Hensler JG. Serotonin. In: Siegel GJ, Agranoff BW, Albers RW, et al., editors. *Basic Neurochemistry: Molecular, Cellular and Medical Aspects*. 6th edition. Philadelphia: Lippincott-Raven; 1999. Available from: <https://www.ncbi.nlm.nih.gov/books/NBK28150/>

Flechsig, P. E. (1920). *Anatomie des menschlichen Gehirns und Rückenmarks auf myelogenetischer Grundlage. v. 1* (Vol. 1). G. Thieme.

Frisina, P. G., Haroutunian, V., & Libow, L. S. (2009). The neuropathological basis for depression in Parkinson's disease. *Parkinsonism & related disorders*, *15*(2), 144–148. <https://doi.org/10.1016/j.parkreldis.2008.04.038>

Giguère, N., Burke Nanni, S., & Trudeau, L. E. (2018). On Cell Loss and Selective Vulnerability of Neuronal Populations in Parkinson's Disease. *Frontiers in neurology*, *9*, 455. <https://doi.org/10.3389/fneur.2018.00455>

Goodman, J. H., Wasterlain, C. G., Massarweh, W. F., Dean, E., Sollas, A. L., & Sloviter, R. S. (1993). Calbindin-D28k immunoreactivity and selective vulnerability to ischemia in the dentate gyrus of the developing rat. *Brain research*, *606*(2), 309–314. [https://doi.org/10.1016/0006-8993\(93\)90999-4](https://doi.org/10.1016/0006-8993(93)90999-4)

Gown AM, de Wever N, Battifora H: Microwave-based antigenic unmasking. A revolutionary technique for routine immunohistochemistry. *Applied Immunohistochemistry* 1(4):256-266, 1993.

Halberstadt, A. L., & Balaban, C. D. (2007). Selective anterograde tracing of the individual serotonergic and nonserotonergic components of the dorsal raphe nucleus projection to the vestibular nuclei. *Neuroscience*, *147*(1), 207–223. <https://doi.org/10.1016/j.neuroscience.2007.03.049>

Halliday GM, Blumbergs PC, Cotton RG, Blessing WW, Geffen LB (1990a). Loss of brainstem serotonin- and substance P-containing neurons in Parkinson's disease. *Brain Res* 510:104–107

Halliday, G. M., Leverenz, J. B., Schneider, J. S., & Adler, C. H. (2014). The neurobiological basis of cognitive impairment in Parkinson's disease. *Movement Disorders*, *29*(5), 634–650.

Halliday GM, Li YW, Blumbergs PC et al (1990b). Neuropathology of immunohistochemically identified brainstem neurons in Parkinson's disease. *Ann Neurol* 27:373–385

Halliday, G. M., & Törk, I. (1986). Comparative anatomy of the ventromedial mesencephalic tegmentum in the rat, cat, monkey and human. *The Journal of comparative neurology*, 252(4), 423–445. <https://doi.org/10.1002/cne.902520402>

Hornung J. P. (2003). The human raphe nuclei and the serotonergic system. *Journal of chemical neuroanatomy*, 26(4), 331–343. <https://doi.org/10.1016/j.jchemneu.2003.10.002>

Huot, P. & Fox, S. H. (2013). The serotonergic system in motor and non-motor manifestations of Parkinson's disease. *Experimental Brain Research*, 230(4), 463–476. <https://doi.org/10.1007/s00221-013-3621-2>

Huot, P., Fox, S. H., & Brotchie, J. M. (2011). The serotonergic system in Parkinson's disease. *Progress in neurobiology*, 95(2), 163–212. <https://doi.org/10.1016/j.pneurobio.2011.08.004>

Karlsson, C., & Karlsson, M. G. (2011). Effects of long-term storage on the detection of proteins, DNA, and mRNA in tissue microarray slides. *The journal of histochemistry and cytochemistry: official journal of the Histochemistry Society*, 59(12), 1113–1121. <https://doi.org/10.1369/0022155411423779>

Kish, S. J., Tong, J., Hornykiewicz, O., Rajput, A., Chang, L. J., Guttman, M., & Furukawa, Y. (2008). Preferential loss of serotonin markers in caudate versus putamen in Parkinson's disease. *Brain: a journal of neurology*, 131(Pt 1), 120–131. <https://doi.org/10.1093/brain/awm239>

Kosofsky, B. E., & Molliver, M. E. (1987). The serotonergic innervation of cerebral cortex: different classes of axon terminals arise from dorsal and median raphe nuclei. *Synapse (New York, N.Y.)*, 1(2), 153–168. <https://doi.org/10.1002/syn.890010204>

Krenacs, L., Krenacs, T., Stelkovic, E., & Raffeld, M. (2010). Heat-induced antigen retrieval for immunohistochemical reactions in routinely processed paraffin sections. *Methods in molecular biology (Clifton, N.J.)*, 588, 103–119. https://doi.org/10.1007/978-1-59745-324-0_14

Magaki, S., Hojat, S. A., Wei, B., So, A., & Yong, W. H. (2019). An Introduction to the Performance of Immunohistochemistry. *Methods in molecular biology (Clifton, N.J.)*, 1897, 289–298. https://doi-org.proxy3.library.mcgill.ca/10.1007/978-1-4939-8935-5_25

Mamounas, L. A., Mullen, C. A., O'Hearn, E., & Molliver, M. E. (1991). Dual serotonergic projections to forebrain in the rat: morphologically distinct 5-HT axon terminals exhibit differential vulnerability to neurotoxic amphetamine derivatives. *The Journal of comparative neurology*, 314(3), 558–586. <https://doi.org/10.1002/cne.903140312>

Mann D M & Yates P O (1983). Pathological basis for neurotransmitter changes in Parkinson's disease. *Neuropathol Appl Neurobiol* 9:3–19

Morgan, J. M., Navabi, H., Schmid, K. W., & Jasani, B. (1994). Possible role of tissue-bound calcium ions in citrate-mediated high-temperature antigen retrieval. *The Journal of pathology*, 174(4), 301–307. <https://doi.org/10.1002/path.1711740410>

Muzerelle, A., Scotto-Lomassese, S., Bernard, J. F., Soiza-Reilly, M., & Gaspar, P. (2016). Conditional anterograde tracing reveals distinct targeting of individual serotonin cell groups (B5-B9) to the forebrain and brainstem. *Brain structure & function*, 221(1), 535–561. <https://doi.org/10.1007/s00429-014-0924-4>

Nielsen, K., Brask, D., Knudsen, G. M., & Aznar, S. (2006). Immunodetection of the serotonin transporter protein is a more valid marker for serotonergic fibers than serotonin. *Synapse (New York, N.Y.)*, 59(5), 270–276. <https://doi.org/10.1002/syn.20240>

Nowinski, W. L. (2020). Evolution of Human Brain Atlases in Terms of Content, Applications, Functionality, and Availability. *Neuroinformatics*, 1–22. <https://doi.org/10.1007/s12021-020-09481-9>

Ohama E & Ikuta F (1976). Parkinson's disease: distribution of Lewy bodies and monoamine neuron system. *Acta Neuropathol* 34:311–319

Okaty, B. W., Freret, M. E., Rood, B. D., Brust, R. D., Hennessy, M. L., deBairos, D., Kim, J. C., Cook, M. N. & Dymecki, S. M. (2015). Multi-Scale Molecular Deconstruction of the Serotonin Neuron System. *Neuron*, 88(4), 774–791. <https://doi.org/10.1016/j.neuron.2015.10.007>

Parent, M., Wallman, M. J., Gagnon, D., & Parent, A. (2011). Serotonin innervation of basal ganglia in monkeys and humans. *Journal of chemical neuroanatomy*, 41(4), 256–265. <https://doi.org/10.1016/j.jchemneu.2011.04.005>

Paulus W & Jellinger K (1991) The neuropathologic basis of different clinical subgroups of Parkinson's disease. *J Neuropathol Exp Neurol* 50:743–755

Poitras, D., & Parent, A. (1978). Atlas of the distribution of monoamine-containing nerve cell bodies in the brain stem of the cat. *The Journal of comparative neurology*, 179(4), 699–717. <https://doi.org/10.1002/cne.901790402>

Raghanti, M. A., Stimpson, C. D., Marcinkiewicz, J. L., Erwin, J. M., Hof, P. R., & Sherwood, C. C. (2008). Differences in cortical serotonergic innervation among humans, chimpanzees, and macaque monkeys: a comparative study. *Cerebral cortex (New York, N.Y.: 1991)*, 18(3), 584–597. <https://doi.org/10.1093/cercor/bhm089>

Ramos-Vara J. A. (2017). Principles and Methods of Immunohistochemistry. *Methods in molecular biology (Clifton, N.J.)*, 1641, 115–128. https://doi-org.proxy3.library.mcgill.ca/10.1007/978-1-4939-7172-5_5

Riekkinen, M., Kejonen, K., Jäkälä, P., Soininen, H., & Riekkinen, P. (1998). Reduction of noradrenaline impairs attention and dopamine depletion slows responses in Parkinson's disease. *European Journal of Neuroscience*, 10(4), 1429-1435.

Sawamoto, N., Piccini, P., Hotton, G., Pavese, N., Thielemans, K., & Brooks, D. J. (2008). Cognitive deficits and striato-frontal dopamine release in Parkinson's disease. *Brain*, *131*(5), 1294-1302.

Sharma, H. M., Kauffman, E. M., & McGaughy, V. R. (1990). Improved immunoperoxidase staining using microwave slide drying. *Laboratory Medicine*, *21*(10), 658-660.

Shi, S. R., Cote, R. J., & Taylor, C. R. (1997). Antigen retrieval immunohistochemistry: past, present, and future. *The journal of histochemistry and cytochemistry: official journal of the Histochemistry Society*, *45*(3), 327–343. <https://doi.org/10.1177/002215549704500301>

Shi, S. R., Key, M. E., & Kalra, K. L. (1991). Antigen retrieval in formalin-fixed, paraffin-embedded tissues: an enhancement method for immunohistochemical staining based on microwave oven heating of tissue sections. *The journal of histochemistry and cytochemistry: official journal of the Histochemistry Society*, *39*(6), 741–748. <https://doi.org/10.1177/39.6.1709656>

Shin, R. W., Iwaki, T., Kitamoto, T., & Tateishi, J. (1991). Hydrated autoclave pretreatment enhances tau immunoreactivity in formalin-fixed normal and Alzheimer's disease brain tissues. *Laboratory investigation; a journal of technical methods and pathology*, *64*(5), 693–702.

Shi, S. R., Shi, Y., & Taylor, C. R. (2011). Antigen retrieval immunohistochemistry: review and future prospects in research and diagnosis over two decades. *The journal of histochemistry and cytochemistry: official journal of the Histochemistry Society*, *59*(1), 13–32. <https://doi.org/10.1369/jhc.2010.957191>

Shimogori, T., Abe, A., Go, Y., Hashikawa, T., Kishi, N., Kikuchi, S. S., Kita, Y., Niimi, K., Nishibe, H., Okuno, M., Saga, K., Sakurai, M., Sato, M., Serizawa, T., Suzuki, S., Takahashi, E., Tanaka, M., Tatsumoto, S., Toki, M., U, M., ... Okano, H. (2018). Digital gene atlas of neonate common marmoset brain. *Neuroscience research*, *128*, 1–13. <https://doi.org/10.1016/j.neures.2017.10.009>

Sigma-Aldrich, Product-MAB5278, Clone PH8, Chemicon®, Mouse
<https://www.sigmaaldrich.com/CA/en/product/mm/mab5278>

Sladek, J. R., Jr, Garver, D. L., & Cummings, J. P. (1982). Monoamine distribution in primate brain-IV. Indoleamine-containing perikarya in the brain stem of *Macaca arctoides*. *Neuroscience*, 7(2), 477–493. [https://doi.org/10.1016/0306-4522\(82\)90281-0](https://doi.org/10.1016/0306-4522(82)90281-0)

Soiza-Reilly, M. & Gaspar, P. (2020). Chapter 2 From B1 to B9: a guide through hindbrain serotonin neurons with additional views from multidimensional characterization. *Handbook of Behavioral Neuroscience*, 31, 23–40. <https://doi.org/10.1016/b978-0-444-64125-0.00002-5>

Stumptner, C., Pabst, D., Loibner, M., Viertler, C., & Zatloukal, K. (2019). The impact of crosslinking and non-crosslinking fixatives on antigen retrieval and immunohistochemistry. *New biotechnology*, 52, 69–83. <https://doi.org.proxy3.library.mcgill.ca/10.1016/j.nbt.2019.05.003>

Sunkin, S. M., Ng, L., Lau, C., Dolbeare, T., Gilbert, T. L., Thompson, C. L., Hawrylycz, M., & Dang, C. (2013). Allen Brain Atlas: an integrated spatio-temporal portal for exploring the central nervous system. *Nucleic acids research*, 41(Database issue), D996–D1008. <https://doi.org/10.1093/nar/gks1042>

Suurmeijer AJH, Boon ME: Notes on the application of microwaves for antigen retrieval in paraffin and plastic sections. *Eur J Morphol* 1993; 31:144-150.

Taber, E., Brodal, A., & Walberg, F. (1960). The raphe nuclei of the brain stem in the cat. I. Normal topography and cytoarchitecture and general discussion. *The Journal of comparative neurology*, 114, 161–187. <https://doi.org/10.1002/cne.901140205>

Tacha, D. & Teixeira, M. (2013). History and Overview of Antigen Retrieval: Methodologies and Critical Aspects. *Journal of Histotechnology*, 25(4), 237–242. <https://doi.org/10.1179/his.2002.25.4.237>

Törk I, Hornung J. P. (1990). Raphe nuclei and the serotonergic system In *The Human Nervous System* Paxinos G, editor. ed. Academic Press; San Diego, CA: 1001–1022.

Vertes, R. P., Linley, S. B., & Hoover, W. B. (2010). Pattern of distribution of serotonergic fibers to the thalamus of the rat. *Brain structure & function*, 215(1), 1–28. <https://doi.org/10.1007/s00429-010-0249-x>

Vogt, C., & Vogt, O. (1919). *Allgemeine ergebnisse unserer hirnforschung* (Vol. 21). JA Barth.

von Economo, C. F., & Koskinas, G. N. (1925). *Die cytoarchitektonik der hirnrinde des erwachsenen menschen*. J. Springer.

Wallman, M. J., Gagnon, D., & Parent, M. (2011). Serotonin innervation of human basal ganglia. *The European journal of neuroscience*, 33(8), 1519–1532. <https://doi.org/10.1111/j.1460-9568.2011.07621.x>

Walther, D. J., Peter, J. U., Bashammakh, S., Hörtnagl, H., Voits, M., Fink, H., & Bader, M. (2003). Synthesis of serotonin by a second tryptophan hydroxylase isoform. *Science (New York, N.Y.)*, 299(5603), 76. <https://doi.org/10.1126/science.1078197>

Wilson, J. M., Levey, A. I., Rajput, A., Ang, L., Guttman, M., Shannak, K., Niznik, H. B., Hornykiewicz, O., Pifl, C., & Kish, S. J. (1996). Differential changes in neurochemical markers of striatal dopamine nerve terminals in idiopathic Parkinson's disease. *Neurology*, 47(3), 718–726. <https://doi.org/10.1212/wnl.47.3.718>

Wilson, M. A., & Molliver, M. E. (1991). The organization of serotonergic projections to cerebral cortex in primates: regional distribution of axon terminals. *Neuroscience*, 44(3), 537–553. [https://doi.org/10.1016/0306-4522\(91\)90076-z](https://doi.org/10.1016/0306-4522(91)90076-z)

Wilson, M. A., & Molliver, M. E. (1991). The organization of serotonergic projections to cerebral cortex in primates: retrograde transport studies. *Neuroscience*, 44(3), 555–570. [https://doi.org/10.1016/0306-4522\(91\)90077-2](https://doi.org/10.1016/0306-4522(91)90077-2)

Wilson, M. A., Ricaurte, G. A., & Molliver, M. E. (1989). Distinct morphologic classes of serotonergic axons in primates exhibit differential vulnerability to the psychotropic drug 3,4-

methylenedioxymethamphetamine. *Neuroscience*, 28(1),
[https://doi.org/10.1016/0306-4522\(89\)90237-6](https://doi.org/10.1016/0306-4522(89)90237-6)

121–137.

Yaziji H, Gown AM: Divalent metal ion chelation is a universal underlying mechanism in heat induced epitope retrieval (abstract). *Modern Pathology* 10(1): 186A, 1997.

Zhang, X., Beaulieu, J. M., Sotnikova, T. D., Gainetdinov, R. R., & Caron, M. G. (2004). Tryptophan hydroxylase-2 controls brain serotonin synthesis. *Science (New York, N.Y.)*, 305(5681), 217. <https://doi.org/10.1126/science.1097540>